Computers and Geotechnics 176 (2024) 106775

Contents lists available at ScienceDirect

Computers and Geotechnics

journal homepage: www.elsevier.com/locate/compgeo

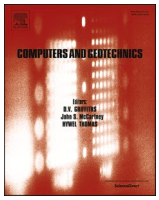

Research Paper

A constitutive model considering the interaction between evolution of microstructure and hydro-mechanical behaviour of unsaturated soils

Tianchi Wu, Peter John Cleall *, Snehasis Tripathy

School of Engineering, Cardiff University, Cardiff, United Kingdom

ARTICLE INFO

Keywords:
Microstructure
Hydro-mechanical behaviour
Constitutive model
Unsaturated soils

ABSTRACT

The evolution of microstructure induced by loading and unloading has a significant impact on the hydro-mechanical behaviour of soils, including volume change, shear strength, water retention and permeability. In this paper, a constitutive model based on the evolution of microstructure is established building on the approach of an existing mechanistic model. In this model, the evolution of microstructure is represented via changes in the pore size distribution (PSD) and assumed to be related solely to the change of void ratio induced by loading and unloading. A PSD-dependent Bishop's effective stress coefficient χ^*, which represents the coupled impact of PSD evolution on hydro-mechanical behaviour of soils, is used to replace the Bishop's effective stress coefficient χ. The model can reproduce and predict the hydro-mechanical behaviour and evolution of microstructure and their interaction within a unified framework. It also has potential in studying the soil-water characteristic curve and multi-field-coupling of soils. Model response and sensitivity analysis are reported based on idealized parameters to give a primary evaluation on the model's performance and feasibility of using PSDs from mercury intrusion porosimetry. It is found that whilst the model is sensitive to parameters representing inter-aggregate pore size distributions it can be satisfactorily applied to represent the hydro-mechanical behaviour and microstructural evolution of unsaturated soils.

1. Introduction

The hydro-mechanical behaviour of unsaturated soils is a long-term research topic (Alonso et al., 2013, 1990; Cai et al., 2018; Davies and Newson, 1992; Fredlund et al., 1978; Fredlund and Morgenstern, 1977; Gens et al., 2006; Lloret-Cabot et al., 2013; Rahardjo et al., 2018; Sheng et al., 2004; Wheeler et al., 2003; Wu et al., 2022) with unsaturated soils behaviour, such as strength and volumetric change, of particular importance in many engineering applications. Many research studies have demonstrated that the microstructure, which can be defined as the arrangement of soil particles and pores (Marshall et al., 1996), can be a significant factor in the behaviour of soils (Alekseeva, 2007; Al-Mukhtar et al., 2012; Alonso et al., 2010; Belnap and Gardner, 1993; Hu et al., 2001; Tsuji et al., 1975; Wang and Bai, 2012). Moreover, strains induced by loading can also lead to the evolution of the microstructure, including changes in pore sizes, pore shapes and pore size distribution. It has been established that the evolution of microstructure significantly influence the hydro-mechanical behaviour of soils and the storage and transmission of liquid, microorganism, chemical substance or other pollutant stored in pores (Izdebska-Mucha et al., 2011; Izdebska-Mucha and Trzciński, 2008; Woignier et al., 2011; Yong, 2003; Zhang, 2005). There exists a strong interrelationship between the hydro-mechanical behaviour of soils and their microstructure and these interactions require investigation and to be represented adequately within theoretical and numerical models.

The impact of microstructure has received considerable attention from many researchers both in terms of experimentally observed behaviour and modelling approaches. Wang and Bai addressed the connection between pore diameter and compressibility of loess noting that compressibility is positively correlated to the proportion of pores larger than 20 μm (Wang and Bai, 2012). Wang et al. studied the impact of microstructure on shear behaviour of natural loess (Wang et al., 2021). They found a correlation between the homogenous deformation, with the increase of confining stresses, and the microstructural evolution of pore shapes changing from angular to rounded. It was also found that the evolution of the macro void ratio can account for the observed dilatancy of unsaturated recompacted and intact loess (Ng et al., 2019). To numerically consider the effect of microstructure, Sanchez et al.

* Corresponding author.
E-mail address: cleall@cardiff.ac.uk (P.J. Cleall).

https://doi.org/10.1016/j.compgeo.2024.106775
Received 12 March 2024; Received in revised form 13 September 2024; Accepted 15 September 2024

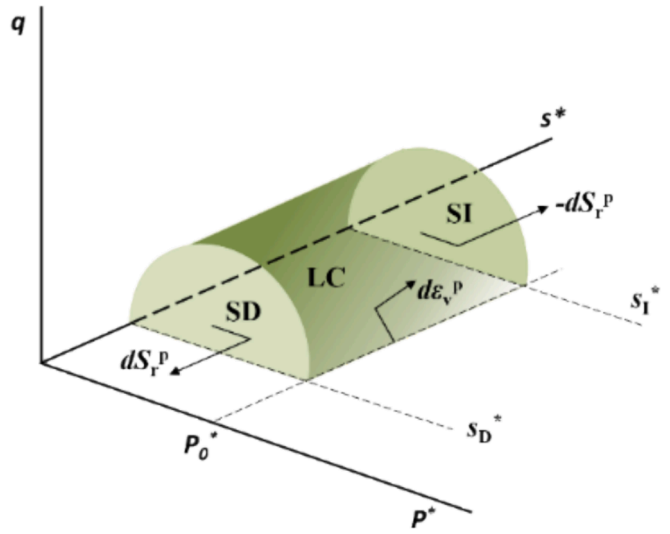

Fig. 1. Yield surfaces of the Glasgow Coupled Model (modified after (Lloret-Cabot et al., 2013)).

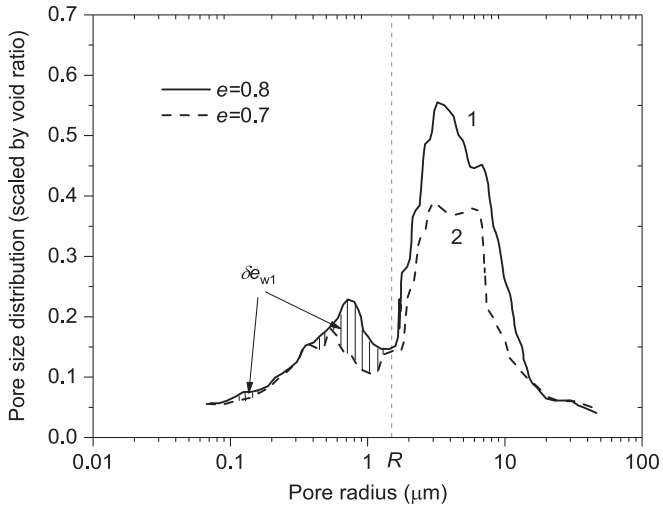

Fig. 2. Illustrations of calculating χ* through pore size distributions (modified after (Vaunat and Casini, 2017)).

Table 1
Framework for the Glasgow Coupled Model (Lloret-Cabot et al., 2013; Wheeler et al., 2003).

Names	Equations	
Stress variable	Bishop's stress tensor: $\xi_{ij}^* = \xi_{ij} - (S_r u_w + (1 - S_r)u_a)\delta_{ij}$	(7)
	Modified suction: $s^* = (u_a - u_w)n$	(8)
Generalized stress/strain increment vectors	$d\tilde{\xi}^* = \left(d\xi_{xx}^*, d\xi_{yy}^*, d\xi_{zz}^*, d\xi_{xy}^*, d\xi_{yz}^*, d\xi_{xz}^*, ds^*\right)^T$	(9)
	$d\tilde{\varepsilon} = \left(d\varepsilon_{xx}, d\varepsilon_{yy}, d\varepsilon_{zz}, d\varepsilon_{xy}, d\varepsilon_{yz}, d\varepsilon_{xz}, -dS_e\right)^T$	(10)
Yield surfaces	$F_{LC} = q^2 - M^2 p^* \left(p_0^* - p^*\right) = 0$	(11)
	$F_{SI} = s^* - s_I^* = 0$	(12)
	$F_{SD} = s_D^* - s^* = 0$	(13)
Coupling among Yield surfaces	$\frac{ds_I^*}{s_I^*} = \frac{ds_D^*}{s_D^*} = k_2 \frac{dp_0^*}{p_0^*}$(Yield on LC)	(14)
	$\frac{dp_0^*}{p_0^*} = k_1 \frac{ds_I^*}{s_I^*} = k_1 \frac{ds_D^*}{s_D^*}$ (Yield on SD/SI)	(15)
Flow rules	$d\tilde{\varepsilon}_j^p = d\lambda_l^j \frac{\partial F_l}{\partial \tilde{\xi}^*}$ with $l = \mathrm{LC}, \beta; j = \mathrm{LC}, \beta, \mathrm{LC} + \beta;$ $\beta = \mathrm{SI}$ or SD	(16)
Hardening laws	$dp_o^* = p_0^* \left[\frac{v d\varepsilon_v^p}{\lambda - \kappa} - \frac{k_1 dS_r^p}{\lambda_s - \kappa_s}\right]$	(17)
	$ds_{I/D}^* = s_{I/D}^* \left[-\frac{dS_r^p}{\lambda_s - \kappa_s} + k_2 \frac{v d\varepsilon_v^p}{\lambda - \kappa}\right]$	(18)
Constitutive relationship	$d\tilde{\xi}^* = \boldsymbol{D}_e^* d\tilde{\varepsilon}^e$(elastic)	(19)
	$d\tilde{\xi}^* = \boldsymbol{D}_e^* d\tilde{\varepsilon}^e = \boldsymbol{D}_{ep}^* d\tilde{\varepsilon}$(elasto-plastic)	(20)

Table 2
Initial states for Speswhite kaolin.

Initial states	Value
p_{net}/kPa	50
s/kPa	300
e	1.208
S_r/%	60.1
p_0^*/kPa	273
S_D^*/kPa	164
S_I^*/kPa	/

Table 3
Model parameters for Speswhite kaolin.

Hydro-mechanical parameters	Value	Pore size distribution and evolution parameters	Value
λ	0.124	a_1	1.198
κ	0.006	σ_1	0.6
λ_s	0.098	μ_1	−1
κ_s	0.0076	a_2	0.01
k_1	0.662	σ_2	0.5
k_2	0.803	μ_2	−5
M	0.71	K_1^1	1
μ	0.3	K_2^1	0.3
G_s	2.6	K_3^1	−0.12
		K_1^2	0
		K_2^2	0
		K_3^2	0

(Sánchez et al., 2005, 2001) selected different constitutive formulations for the macrostructural level and the microstructural level. An interaction formulation was proposed to connect these two levels and establish a microstructurally dependent model. This model was validated against experimental data from tests conducted by Lloret et al on heavily compacted bentonite (Lloret et al., 2003). Wu et al. adopted the effective degree of saturation as microstructural index and established a hydro-mechanical coupled model that considers the microstructure (Wu et al., 2022). The use of effective degree of saturation ignores the effect of water stored in micropores which contributes little to the effective stress (Alonso et al., 2010). Others have also explored microstructural effects in unsaturated soil behaviour. Pasha et al. explored the dependency of the water retention curve (WRC) on void ratio and proposed a model for WRC with hysteresis considered (Pasha et al., 2017). Russell and Buzzi (2012) adopted a fractal method that considers the microstructure as a successive orders of pores and throats with different sizes when building a soil–water characteristic model. According to thermodynamic theory, both Jiang et al. (2017) and Nikooee et al. (2013) proposed microstructure-dependent equations for Bishop's effective stress coefficient. In each case the evolution of microstructure is not represented by the model and only the fractal method directly considers microstructure.

The evolution of microstructure, often reported in terms of changes in pore size distribution, induced by hydro-mechanical loading has been investigated by a number of researchers (Li and Zhang, 2009; Oualmakran et al., 2016; Thom et al., 2007; Vaunat and Casini, 2017). The pore size distribution, which can be considered as a microstructural index, is highly sensitive to compaction conditions and the change of the void ratio during a loading process (Gao et al., 2020; Li et al., 2021; Niu et al., 2021; Qian et al., 2022; Vaunat and Casini, 2017). For soils with

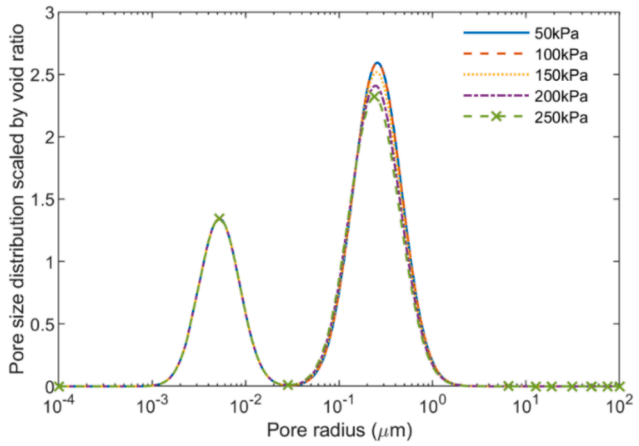

Fig. 3. Initial pore size distribution and its evolution under idealized parameters.

double porosity the pore size distribution related to micropores is usually unaffected by compaction or void ratio change with most compression occurring within the macropores (Li and Zhang, 2009; Wang et al., 2020, 2019; Yu et al., 2016).

A review of the literature suggested that the compressibility, swelling, shear strength and water retention behaviour of unsaturated soils have been studied based on the microstructure information. In the reported studies the microstructure of soils has been represented by either the void ratio or the effective degree of saturation, or even the pore size distribution. A wider application of the microstructure-based approaches, such as contaminant transport, landfill and pavement design require establishing the evolution of the pore-size distribution due to loading/unloading, which has not been explicitly considered in the literature.

The paper initially introduces the evolution of pore size distribution and its dependency on the change of the void ratio (loading), with the pore size distribution represented by a normal or log-normal distribution through a fitting method (Ghabezloo et al., 2021; Li and Zhang, 2009; Romano et al., 2011; Yu et al., 2016). After the fitting parameters are determined, the relationship between the void ratio and the fitting parameters can be studied. An approach based on the Glasgow Coupled Model (GCM) (Lloret-Cabot et al., 2013; Wheeler et al., 2003) is then

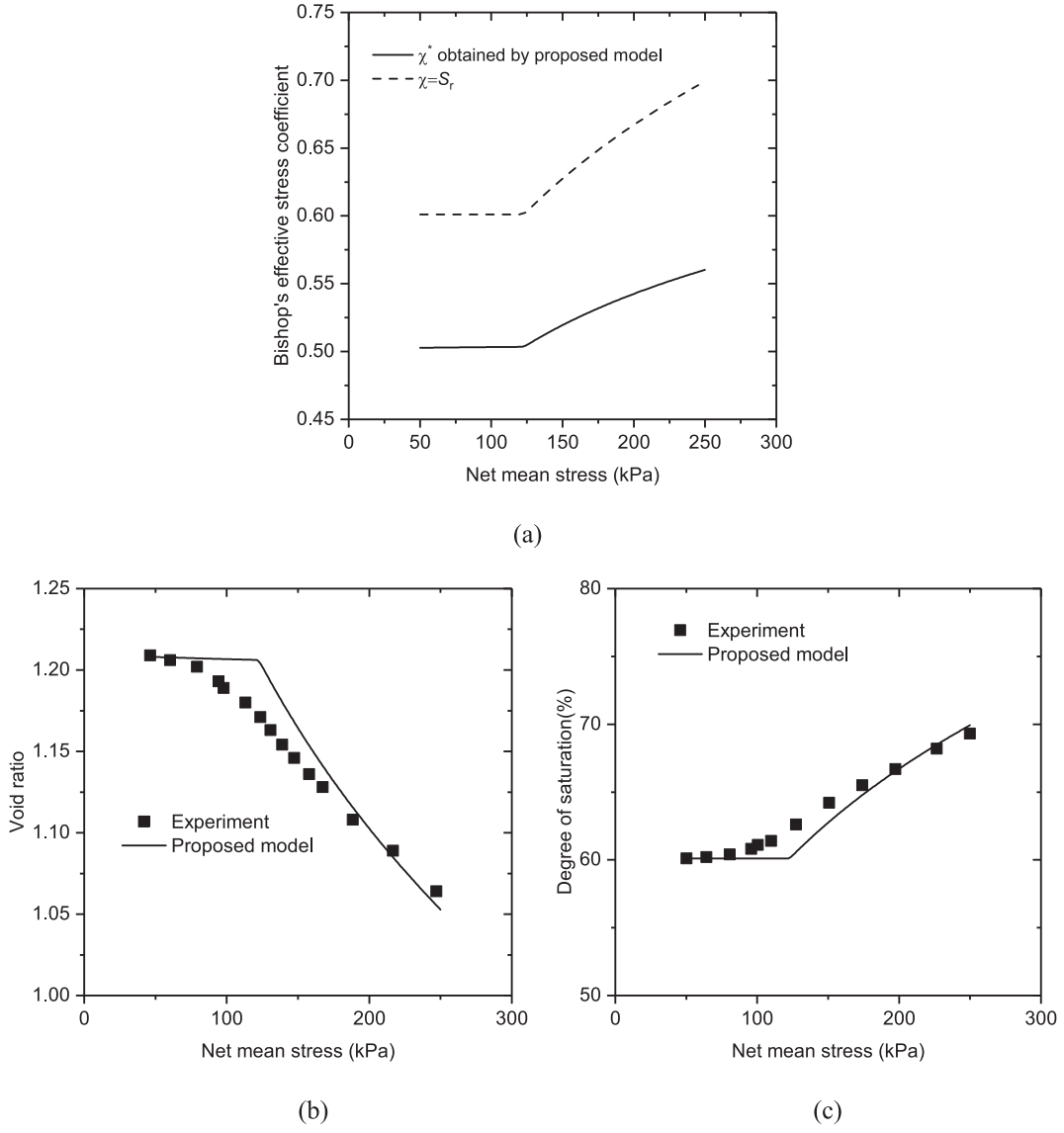

Fig. 4. Comparison between model response and experimental results: (a) Bishop's effective stress coefficient; (b) Void ratio; (c) Degree of saturation.

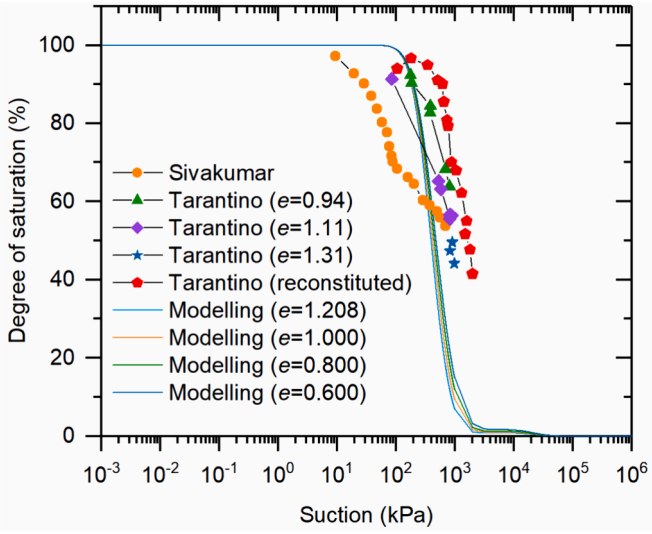

Fig. 5. Comparison in SWCCs between modelling and experimental results.

adopted to represent the macro structural stress–strain behaviour (in terms of void ratio) of unsaturated soils. The impact of the macro-structural hydro-mechanical behaviour on the microstructure is hitherto established. In the past, the GCM has been used to study the hydro-mechanical behaviour of unsaturated soils including the effects of hysteresis in drying and wetting (Wheeler et al., 2003). It has been recognised that the GCM has a successful interpretation in coupling the mechanical behaviour with the hydraulic behaviour and the stress–-strain response is satisfactorily determined by using this model (Gallipoli et al., 2003; Lloret-Cabot et al., 2013; Wheeler et al., 2003). Some studies have identified that the GCM has limitations, such as the difficulty in experimentally calibrating the synchronized evolution of the yield surfaces (Sheng and Zhou, 2011) and it has been unable to take into account the simultaneous flow of air and water and their complex interaction with the deformation of the solid skeleton within a consistent elasto-plastic framework (Khalili et al., 2008). However, the use of the GCM in the current study is primarily to establish the stress–strain response of unsaturated soils and hence the limitations on the use of this model do not affect the outcomes of the investigation.

To realize the interaction between the macrostructural hydro-mechanical behaviour and the microstructure, a PSD-dependent

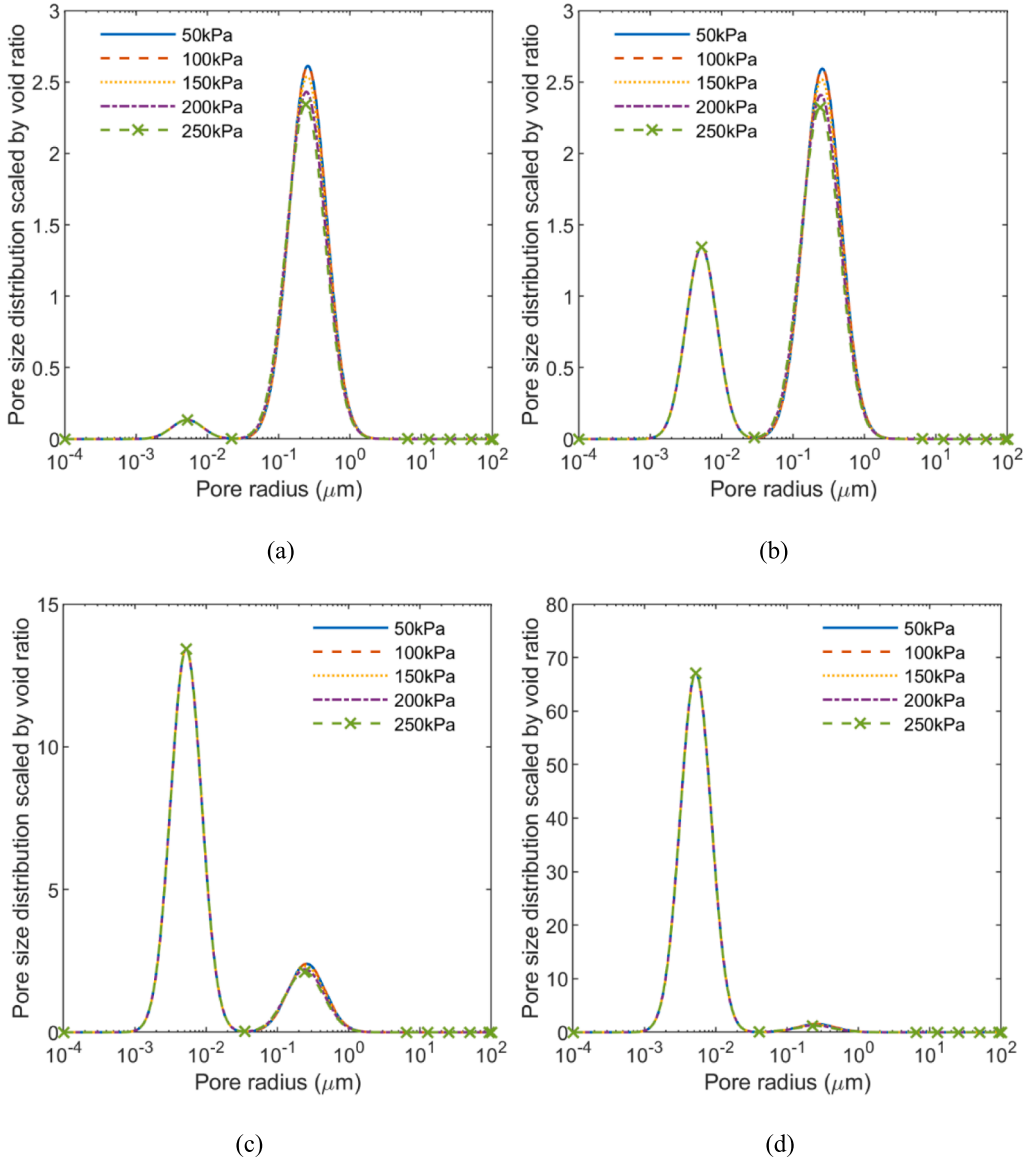

Fig. 6. Evolution of pore size distributions under various a_2: (a) $a_2 = 0.001$; (b) $a_2 = 0.01$; (c) $a_2 = 0.1$; (d) $a_2 = 0.5$.

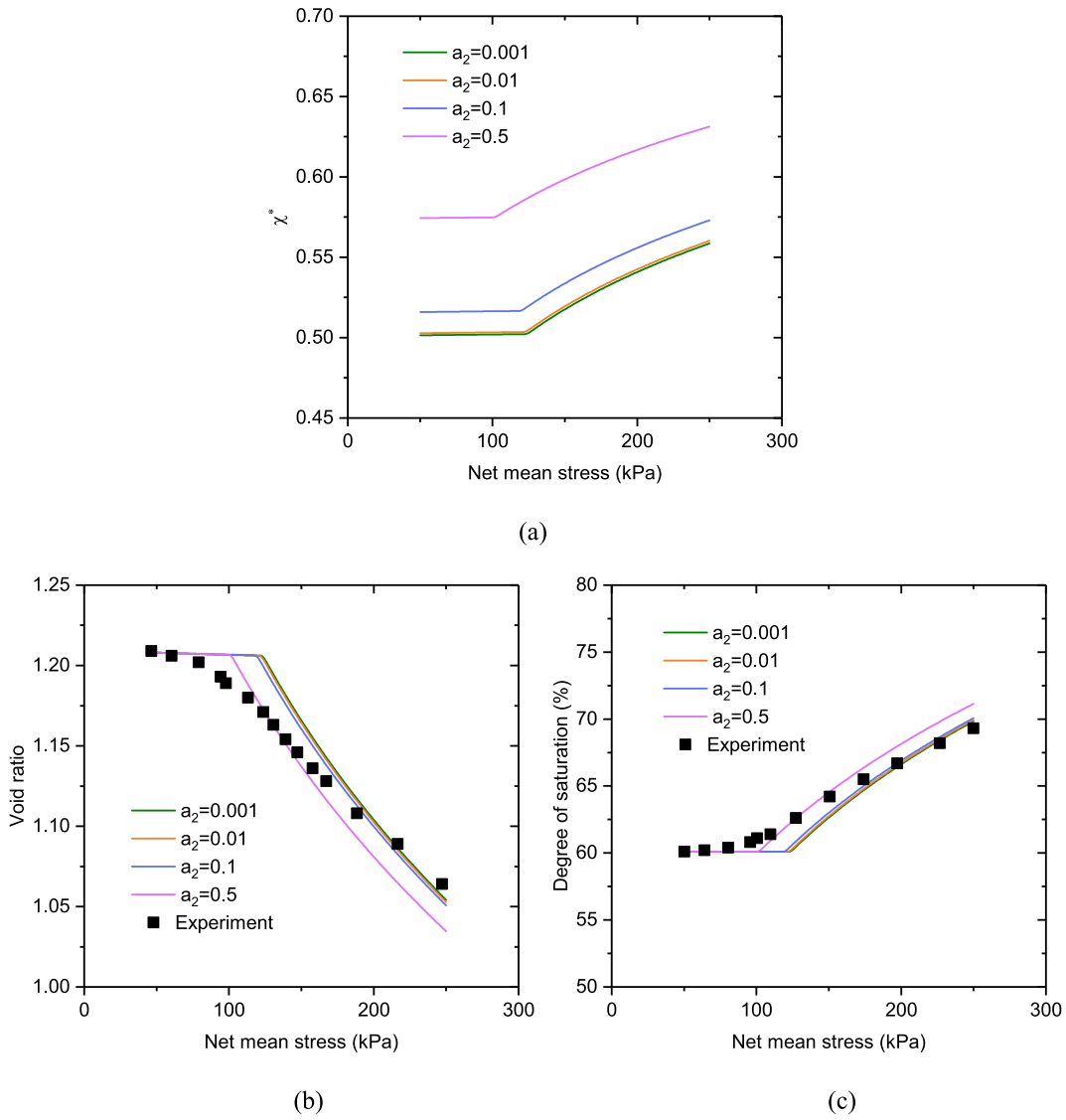

Fig. 7. Model sensitivity to a_2: (a) Bishop's effective stress coefficient; (b) Void ratio; (c) Degree of saturation.

Bishop's effective stress coefficient, termed here as χ^*, proposed by Vaunat and Casini (2017a) is adopted. The PSD-dependent χ^* is established based on work input theory which gives χ^* both a thermodynamic basis and a physical meaning. However, while the common Bishop's effective stress coefficient χ is usually assumed to be related to the degree of saturation in constitutive modelling (Lloret-Cabot et al., 2013; Musso et al., 2020; Nuth and Laloui, 2008; Wheeler et al., 2003; Wu et al., 2022; Zhang and Lu, 2020), the PSD-dependent χ^* has only been applied in constitutive models in a limited way (Niu et al., 2021; Vaunat and Casini, 2017).

In this paper, the performance of PSD-dependent χ^* is for the first time evaluated in a constitutive model. The adoption of the PSD-dependent χ^* enables the model to reproduce the stress–strain behaviour, water retention behaviour and the evolution of microstructure of unsaturated soils in a unified framework, which has not been explicitly studied in the past. Due to the lack of experimental evidence related to PSD evolution of samples undergoing a triaxial shear loading path, model response in an isotropic loading condition is explored, based on both published and idealized parameters, to investigate the model's performance in representing hydro-mechanical behaviour and microstructural evolution. Comparisons between the model and experimental results from previously reported tests on Speswhite kaolin are also made. The sensitivity analysis is also presented in order to investigate the feasibility of using PSDs obtained by Mercury Intrusion Porosimetry (MIP) in this model, considering that the PSDs obtained by MIP and the fitted PSDs cannot be fully representative of the microstructure (Gao et al., 2020; Wang et al., 2020).

2. Evolution of pore size distribution

Pore size distribution is a microstructure-based measure based on pore sizes and their relative proportions to overall pore volume. It can be experimentally estimated by Mercury Intrusion Porosimetry (MIP) (Delage et al., 1996; Delage and Lefebvre, 1984; Gane et al., 2004; Lawrence, 1978; Nagpal et al., 1972; Ninjgarav et al., 2007; Sridharan et al., 1971). There are three main ways to represent pore size distribution, namely the cumulative pore size distribution, incremental pore size distribution and differential pore size distribution (Nagpal et al., 1972; Ninjgarav et al., 2007; Sridharan et al., 1971). Assuming the cumulative pore size distribution curve can be described by a function $F(r)$ where r is the radius of pore size, the differential pore size distribution then can be defined as:

$$f(r) = \frac{\mathrm{d}F(r)}{\mathrm{d}r} \text{ or } f(r) = \frac{\mathrm{d}F(r)}{V_s \mathrm{d}r} \text{ (scaled by void ratio)} \quad (1)$$

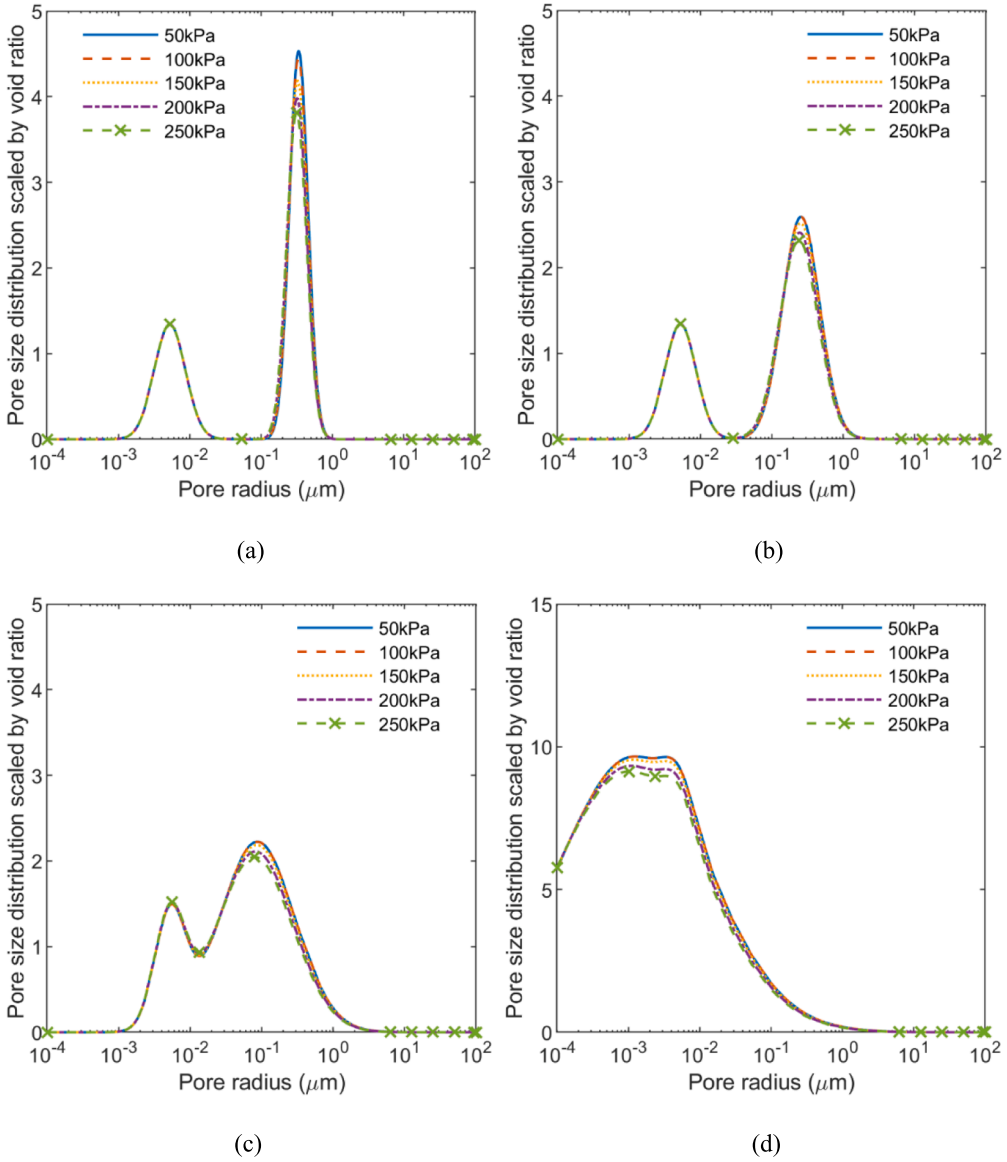

Fig. 8. Evolution of pore size distributions under various σ_1: (a)$\sigma_1 = 0.3$; (b)$\sigma_1 = 0.6$; (c)$\sigma_1 = 1.2$; (d)$\sigma_1 = 2.4$.

where V_s is the total solid volume per unit of weight (dried sample).

According to the number of peaks in pore size distribution, the differential pore size distribution can be classified into three types, including unimodal, bimodal and trimodal distributions (Burger and Shackelford, 2001; Burton et al., 2014; Satyanaga, 2013; Wang et al., 2020; Zhou et al., 2017). A bimodal distribution will have two distinct peaks corresponding to inter-aggregate pores (macropores) and intra-aggregate pores (micropores), respectively.

The microstructure will evolve during a loading/unloading process. The evolution occurs in the variation of the dominant pore size, the volumetric proportions of pores of different sizes and the geometric form of pore size distribution. There is significant evidence to show that the evolution of microstructure and pore size distribution is highly correlated to changes in void ratio (Cai et al., 2020; Li et al., 2021; Li and Zhang, 2009; Yu et al., 2016). To quantitively study the relationship between pore size distribution and void ratio, the pore size distribution is often defined or fitted by a normal distribution or log-normal distribution. Since bimodal and trimodal distribution have more peaks, they can be described by multiple normal (log-normal) distributions, hence the pore size distribution can be represented, for example, as (Li et al., 2020; Li and Zhang, 2009):

$$f(r) = \sum_{i=1}^{j} \frac{a_i}{\sqrt{2\pi}\sigma_i} \exp\left(-\frac{(r-\mu_i)^2}{2\sigma_i^2} \right) (Normal\ distribution) \tag{2}$$

or

$$f(r) = \sum_{i=1}^{j} \frac{a_i}{\sqrt{2\pi}\sigma_i r} \exp\left(-\frac{(\ln(r)-\mu_i)^2}{2\sigma_i^2} \right) (Log-normal\ distribution) \tag{3}$$

where i and j are related to the type of pore size distribution, unimodal ($j = 1$), bimodal ($j = 2$) or trimodal ($j = 3$) and a_i, μ_i and σ_i are fitting variables for the distributions. The relationship between these parameters and void ratio can be used to represent the evolution of pore size distribution during loading.

After obtaining the parameters at different void ratios by fitting experimental data, the evolution of pore size distributions with changing void ratios can also be acquired by a fitting method. Assuming that the change of each parameter is linearly related to the change of void ratio, the variation of parameters can be defined as:

$$\Delta a_i = K_1^i \Delta e \tag{4}$$

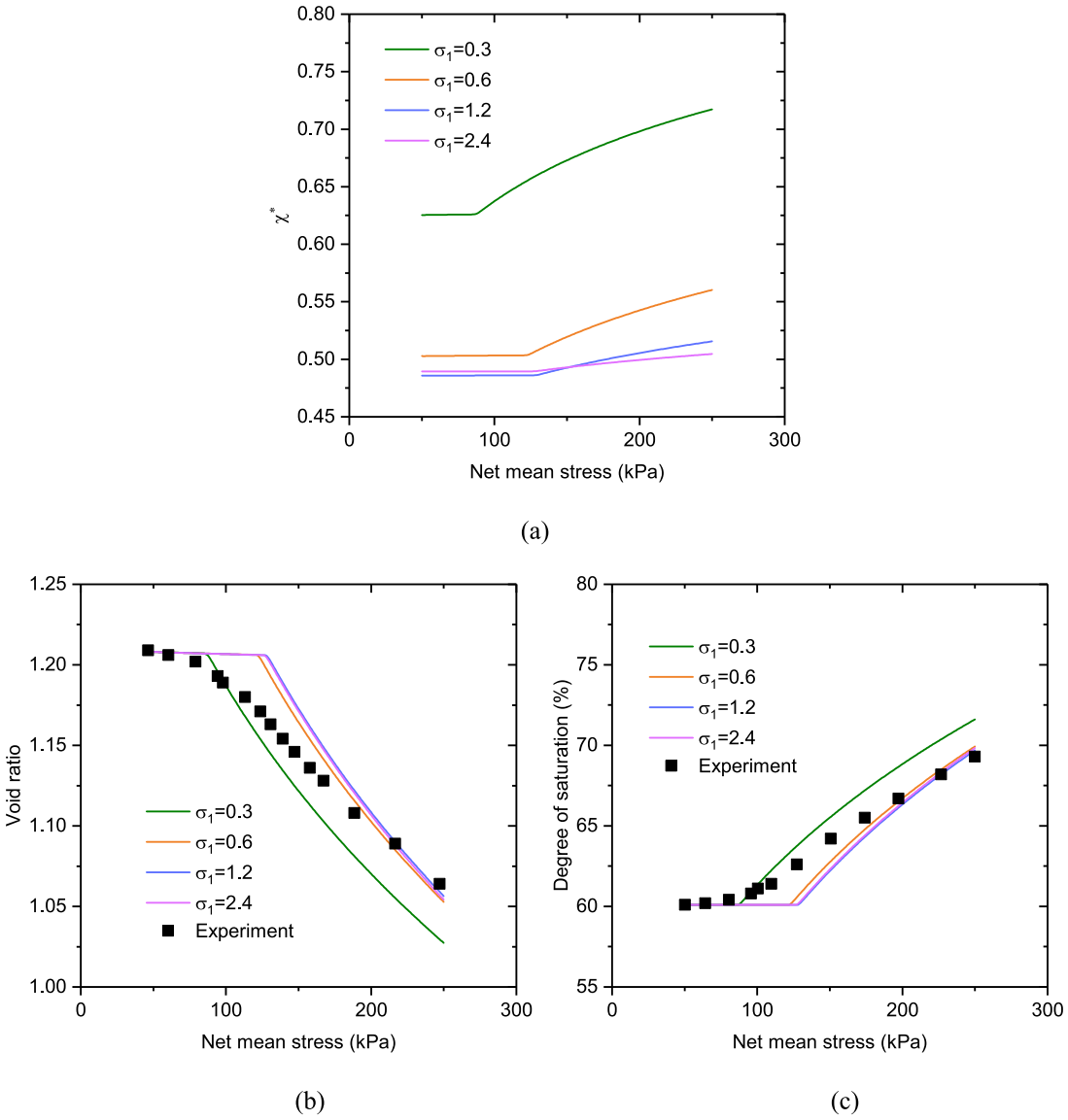

Fig. 9. Model sensitivity to σ_1: (a) Bishop's effective stress coefficient; (b) Void ratio; (c) Degree of saturation.

$$\Delta\mu_i = K_2^i \Delta e \tag{5}$$

$$\Delta\sigma_i = K_3^i \Delta e \tag{6}$$

where K_1^i, K_2^i and K_3^i are fitting parameters. The relationship between these parameters and the void ratio can also be taken to be nonlinear depending on the geometric features of experimental results in a parameter-void ratio graph (Li et al., 2020; Li and Zhang, 2009). Since the change of void ratio can be readily calculated by a traditional constitutive model, it is proposed here to use a constitutive model to reproduce and predict the evolution of pore size distribution.

3. Basic framework for hydro-mechanical behaviour

The representation of the macro structural stress–strain behaviour of unsaturated soils in the proposed model is established following the approach proposed in the Glasgow Coupled Model (GCM) (Lloret-Cabot et al., 2013; Wheeler et al., 2003). The GCM is a hydro-mechanical constitutive model that considers the effect of degree of saturation on mechanical behaviour via use of Bishop's effective stress (Bishop, 1959) and modified suction as stress variables. The generalized stress, strain increment vectors and Modified Camclay Model (MCC) are selected to extend the model to three-dimensional triaxial space. The GCM, which does not explicitly consider the impact of microstructure, has three yield surfaces, including the loading-collapse surface (LC), suction increase surface (SI) and suction decrease surface (SD), as shown in Fig. 1. It is assumed that the three yield surfaces are fully coupled to each other, which means yielding on each one of three yield surfaces will induce the coupled movement of the other two surfaces.

The basic framework for the GCM is presented in Table 1. Eight parameters are included in GCM, namely the slope of normal consolidation line λ, slope of rebound curve κ, coupling parameters for yield surfaces k_1 and k_2, the slope of critical state line M, the slope of the main drying curve λ_s, the slope of the main wetting curve κ_s and Poisson's ratio μ. In the framework of GCM, ξ_{ij} is the stress tensor; $d\varepsilon_{ij}$ is the strain increment tensor; δ_{ij} is the Kronecker delta; u_w is the water pressure; u_a is the air pressure; S_r is the degree of saturation and n is the porosity; $d\lambda_l^j$ is the plastic multiplier with j related to the plastic mechanism which is active (e.g. when yield on LC yield surface is activated j is LC and for yield on SI or SD j is LC is β) and l is associated with plastic changes of effective degrees of saturation (when l is β) or volumetric strains (when l is LC); $\boldsymbol{D}_e^*$ is the generalized elastic matrix and $\boldsymbol{D}_{ep}^*$ is the generalized

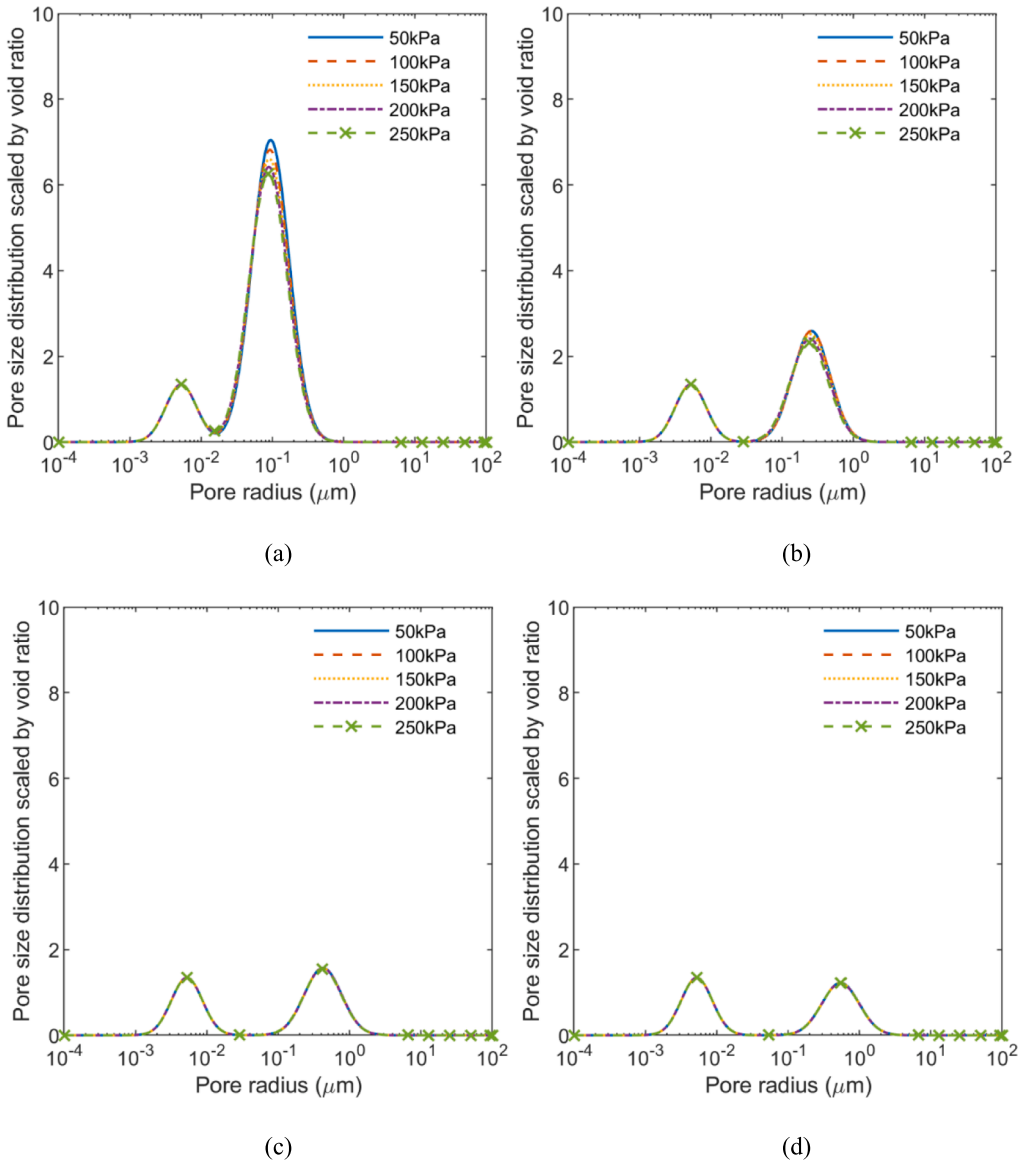

Fig. 10. Evolution of pore size distributions under various μ_1: (a)$\mu_1 = -2$; (b)$\mu_1 = -1$; (c)$\mu_1 = -0.5$; (d)$\mu_1 = -0.25$.

elasto-plastic matrix.

4. Interaction between the evolution of the microstructure and the hydro-mechanical behaviour

Here, a constitutive model that considers the interaction between the evolution of the microstructure and the hydro-mechanical behaviour is proposed. It has been indicated that the evolution of pore size distribution can be reproduced or predicted by the change of void ratio (Gramegna, 2022; Li et al., 2020; Li and Zhang, 2009) if a specific constitutive model is selected and the loading path is predetermined. However, this only considers how the loading can induce the evolution of pore size distribution and does not address how the variation of microstructure affects the mechanical behaviour of soils. The impact of changing microstructure can be studied through the incremental work input per unit volume during loading (Vaunat and Casini, 2017):

$$\delta w = -p\frac{\delta V}{V} + u_w\frac{\delta V_w}{V} + u_a\frac{\delta V_a}{V} \tag{21}$$

where V is the total volume; p is the total mean stress; u_w is the water pressure;u_a is the air pressure; V_w is the water volume; V_a is the air volume. δ represents the change of volume. This expression is based on the approach of Houlsby (1997), who assumed that the air water interface moves with the soil skeleton and so disappears from the expression given. Considering that the solid is incompressible, the change of volume is equal to the change of pore volume δV_V and is composed of the changes of both water volume and air volume:

$$\delta V = \delta V_V = \delta V_w + \delta V_a \tag{22}$$

The change of water volume can also be separated into two components δV_{w1} and δV_{w2}:

$$\delta V_w = \delta V_{w1} + \delta V_{w2} = \chi^* \delta V_V + \delta V_{w2} \tag{23}$$

δV_{w1} is the water volume change generated by the change of pore volume and it is assumed to be proportional to the total change of pore change through a proportionality coefficient χ^*. δV_{w2} is the water volume change induced by the change of suction. By substituting (22) and (23) into (21), the work input can be expressed as:

$$\delta w = -[p - \chi^* u_w - (1-\chi^*)u_a]\frac{\delta V}{V} - (u_a - u_w)\frac{\delta V_{w2}}{V} \tag{24}$$

Since $\frac{\delta V}{V}$ is the volumetric strain increment, then equation (24) can

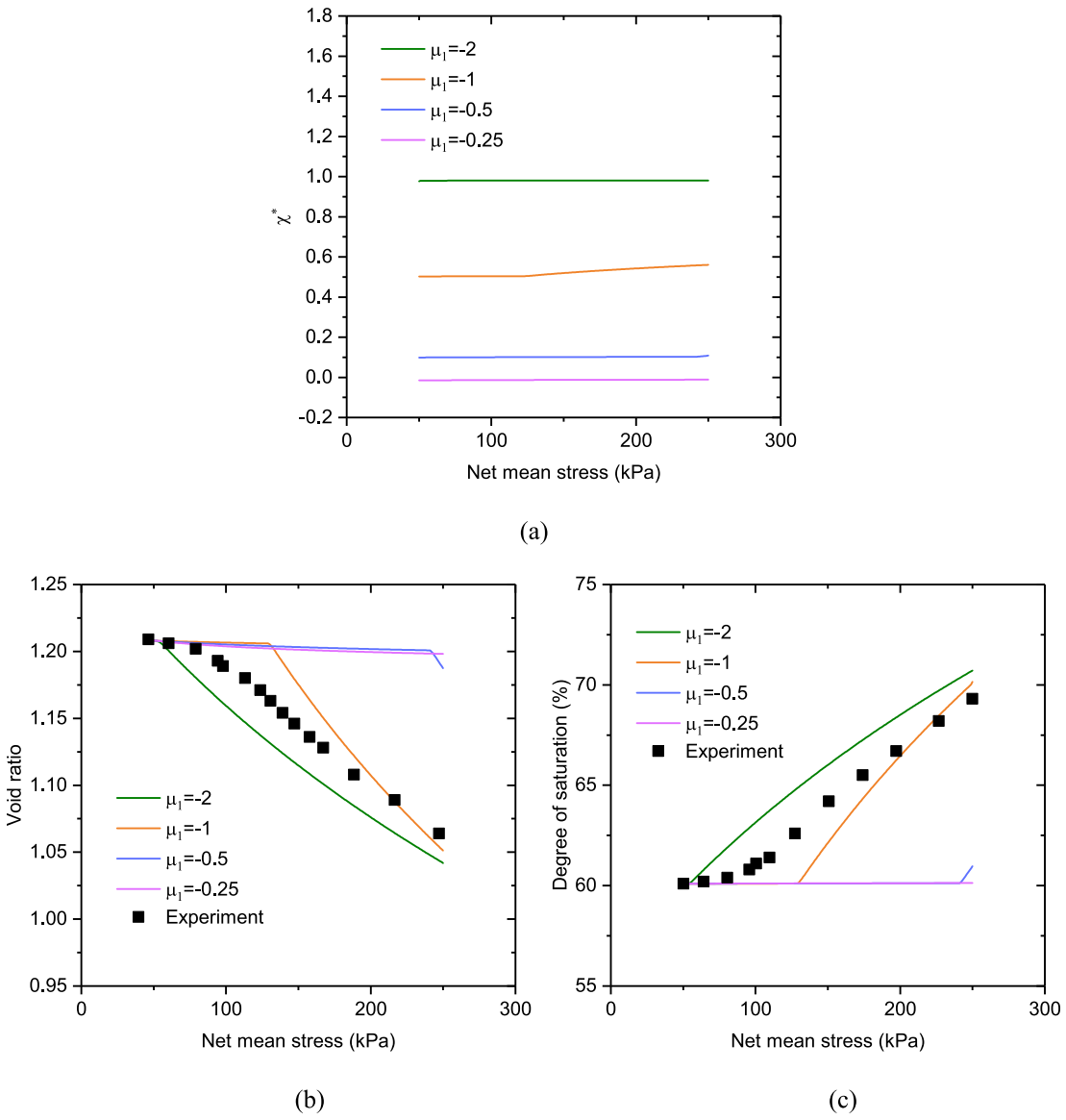

Fig. 11. Model sensitivity to μ_1: (a) Bishop's effective stress coefficient; (b) Void ratio; (c) Degree of saturation.

also be expressed as:

$$\delta w = -[p - \chi^* u_w - (1-\chi^*)u_a]\delta\varepsilon_V - (u_a - u_w)\frac{\delta V_{w2}}{V} \tag{25}$$

It can be noticed that the term '$[p - \chi^* u_w - (1-\chi^*)u_a]$' is consistent with the Bishop's effective stress expression (Bishop, 1959). Therefore, the proportionality coefficient χ^* can also serve as the Bishop's effective stress coefficient. The coefficient χ^* is defined as (Vaunat and Casini, 2017):

$$\chi^* = \frac{\delta V_{w1}}{\delta V_V} = \frac{\delta e_{w1}}{\delta e} \tag{26}$$

where e_{w1} is the water ratio (the ratio of water volume to soil solid volume) at constant suction and e is the void ratio. To obtain the coefficient χ^*, the change of void ratio δe can be easily acquired by a constitutive model. The change of water ratio δe_{w1} can be determined via consideration of the pore size distribution (scaled by the void ratio). Fig. 2 presents two pore size distribution curves at two different void ratios presented by Vaunat and Casini (2017). Curve 1 is compressed to Curve 2 in a loading path where the void ratio decreases from 0.8 to 0.7. The pore size distributions have been scaled by the void ratio, so the area below each curve is equal to the void ratio. The difference in total area between these two curves is the change of void ratio δe. Since water is stored in pores, if the volume of pores fully filled with water can be determined, the water volume and so the water ratio can be obtained. According to capillary theory and Washburn's equation (Washburn, 1921), there exists a largest pore size that the liquid can reach and every pore that has a smaller pore size will be fully filled. The equation for the largest pore size is defined as:

$$R = \frac{2\gamma\cos\theta}{s} \tag{27}$$

where R is the pore radius; γ is the surface tension of water; θ is the contact angle between water and pore wall (assumed to be 0) (Fredlund and Rahardjo, 1993; Fredlund and Xing, 1994) and s is the suction. Once R is determined, the water volume is equivalent to the pore volume of pores smaller than R and so the water ratio is equivalent to the void ratio of pores smaller than R. The area difference within the range that radius is smaller than R between Curve 1 and Curve 2 is the change of water ratio δe_{w1}. Then the coefficient χ^* can be calculated from:

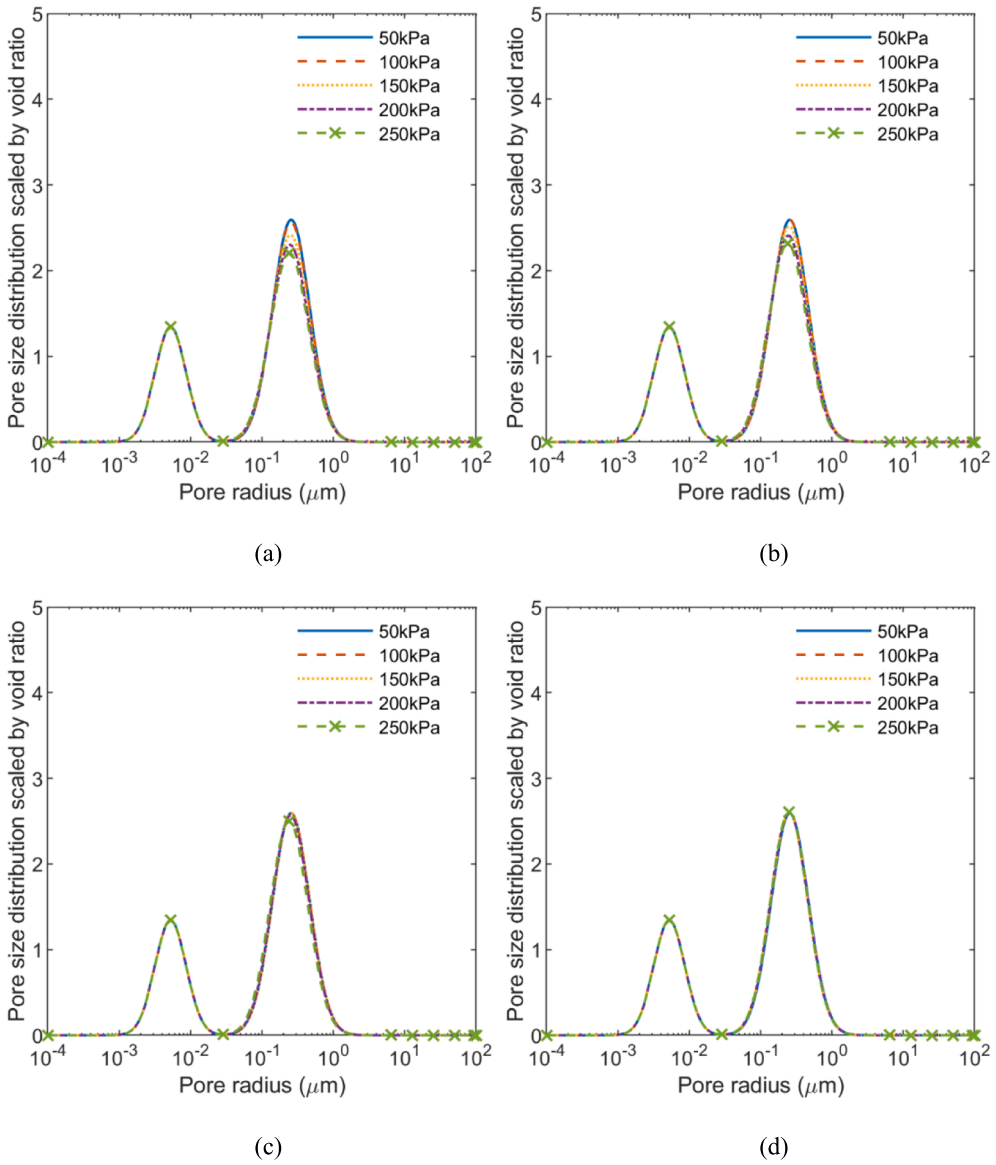

Fig. 12. Evolution of pore size distributions under various K_2^1: (a)$K_2^1 = 0.15$; (b)$K_2^1 = 0.3$; (c)$K_2^1 = 0.6$; (d)$K_2^1 = 1.2$.

$$\delta e_{w1} = \int_0^R [\mathrm{PSD}_1(r) - \mathrm{PSD}_2(r)]\mathrm{d}r \tag{28}$$

$$\chi^* = \frac{\delta e_{w1}}{\delta e} = \frac{\int_0^R [\mathrm{PSD}_1(r) - \mathrm{PSD}_2(r)]\mathrm{d}r}{\delta e} \tag{29}$$

Since the coefficient χ^* can be calculated via consideration of pore size distribution evolution and it is also an important stress variable in a constitutive model, a relationship between the variation of pore size distribution (microstructure) and the behaviour of a constitutive model can be established. The evolution of the pore size distribution is assumed to be solely related to the void ratio, which can be calculated by the constitutive model, while the pore size distribution-dependent coefficient χ^* is adopted in the model to consider the effect of the microstructural evolution on the effective stress and hydro-mechanical behaviour. Adopting the GCM as the basic framework for the hydro-mechanical behaviour and using log-normal distributions to describe the pore size distribution and its evolution, has allowed the establishment of a model that can represent the stress–strain behaviour, the hydraulic behaviour, the evolution of the microstructure and the interaction among them within the same framework.

Since pore size distribution and its evolution is considered, this model also has the potential of studying soil–water characteristic curve (SWCC) and the effects of microstructure on other multi-field-coupling behaviour of soils. Many researchers have predicted the SWCC based on its physical relationship with PSD (Della Vecchia et al., 2015; Li and Vanapalli, 2021; Simms and Yanful, 2004). Since this model can estimate the PSDs at various void ratios, SWCCs at various ratios can also be calculated from the results of the model. Furthermore due to the interaction between PSD, volume change, water content, heat and chemical reaction, this model also has the potential to be further extended to consider the thermo-chemical-hydro-mechanical coupling of soils (Bai et al., 2021, 2020).

5. Model response and sensitivity analysis

In this section a representative example is presented to demonstrate model performance and sensitivity. In particular, the hydro-mechanical behaviour of Speswhite kaolin is considered during a loading path experimentally reported by (Lloret-Cabot et al., 2013). The parameters related to the hydro-mechanical behaviour were adopted from experimental results reported by (Lloret-Cabot et al., 2013). The parameters

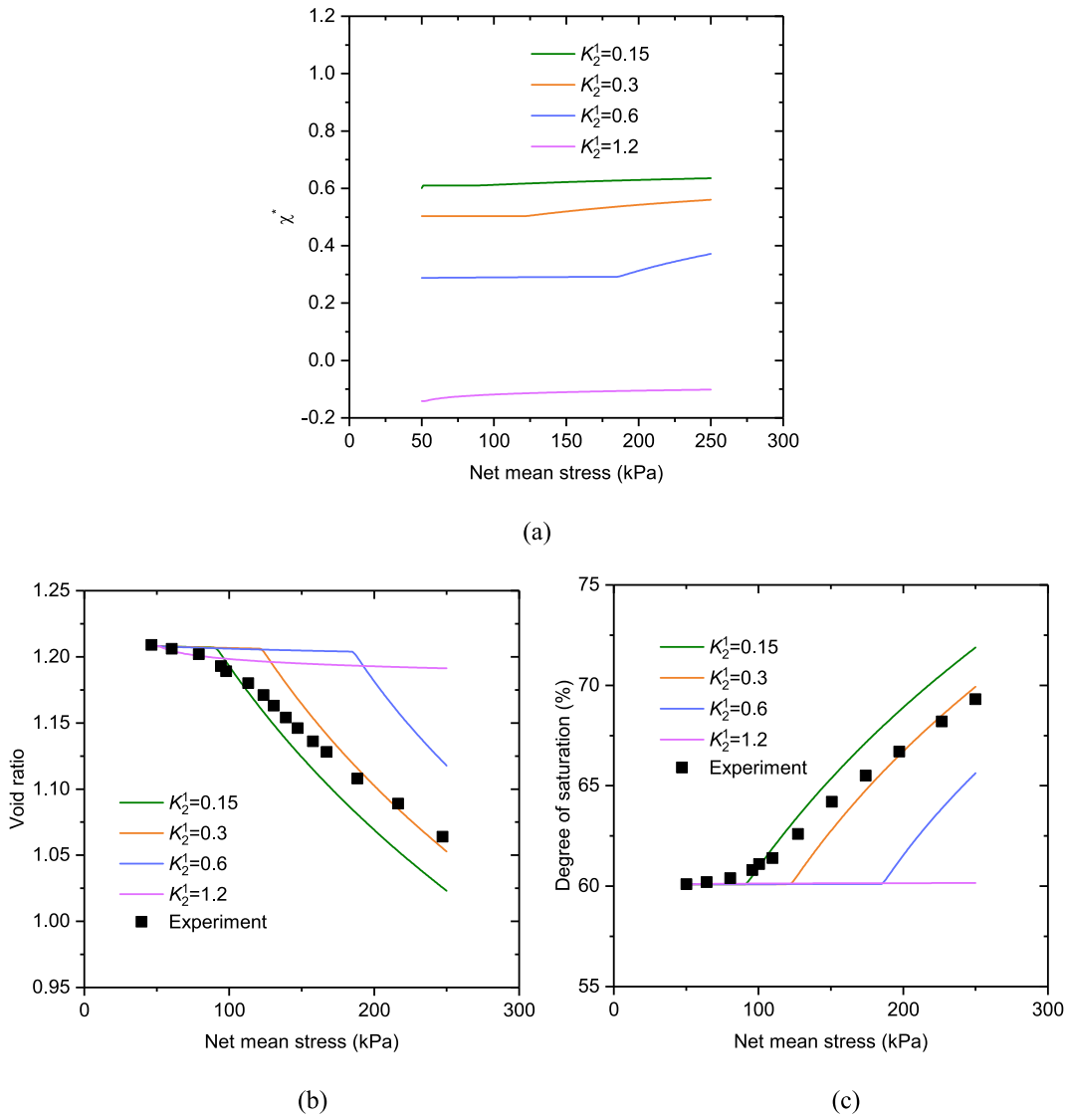

Fig. 13. Model sensitivity to K_2^1: (a) Bishop's effective stress coefficient; (b) Void ratio; (c) Degree of saturation.

for the initial pore size distribution are determined based on the experimental soil–water characteristic curve (SWCC) of Speswhite kaolin reported by Tripathy et al. (Tripathy et al., 2014). According to (Tripathy et al., 2014), the SWCC of Speswhite kaolin starts to have a significant change of degree of saturation at a suction of about 400 kPa, this can be assumed as being the suction at which the largest pores are being evacuated and so can be used to infer the largest pore size of the PSD. According to Young-Laplace equation, the equivalent pore radius at this suction is 0.35 μm. Since the reported void ratio at this suction is 0.9 and the initial void ratio adopted for modelling is 1.208, it is reasonable to assume that the initial PSD will have macropores larger than 0.35 μm, and hence the pore radius at peak density is assumed to be around 0.35 μm. Also to ensure consistency, the area below the selected initial pore size distribution is set to be equal to the initial void ratio of 1.208. It is recognised that due to the limitation of MIP, in which mercury fails to fully inundate very large pores and cannot intrude very small pores (leading to a measuring range usually from several nanometres to several hundred micrometres), the pore size distribution obtained from MIP cannot fully represent all pores of soils. Therefore, the intruded void ratio e_{in} can be smaller than the actual void ratio e (Wang et al., 2020) and calibration and modification of the pore size distribution shall be implemented to ensure consistency in modelling.

Due to a lack of experimental evidence (i.e. MIP data) parameters concerning the evolution of pore size distributions were selected by means of the enumeration method to achieve physically meaningful results. All parameters selected are within a reasonable range and result in pore size distributions that have similar geometric shapes and evolutional features as those of reported by others (Burton et al., 2014; Li and Zhang, 2009; Thom et al., 2007; Vaunat and Casini, 2017). Based on the previously adopted parameters, a sensitivity analysis was then conducted by changing several PSD-related parameters to study the impact of these parameters on the modelled pore size distribution evolution and hydro-mechanical behaviour.

An isotropic loading path with an increase in net mean stress from 50 kPa to 250 kPa was considered. The suction remained constant at 300 kPa during this loading. The initial states and parameters for Speswhite kaolin are presented below (see Table 2 and Table 3). The parameters for hydro-mechanical behaviour are derived from reported experimental results on Speswhite kaolin (Lloret-Cabot et al., 2013; Sivakumar, 1993). The pore size distribution of Speswhite kaolin is assumed to have bimodality where the soil pores can be classified into inter-aggregate pores (macropores) and intra-aggregate pores (micropores), so the formula for the PSD is:

$$f(r) = \frac{a_1}{\sqrt{2\pi}\sigma_1 r}\exp\left(-\frac{\ln(r)-\mu_1}{2\sigma_1^2}\right) + \frac{a_2}{\sqrt{2\pi}\sigma_2 r}\exp\left(-\frac{\ln(r)-\mu_2}{2\sigma_2^2}\right) \quad (30)$$

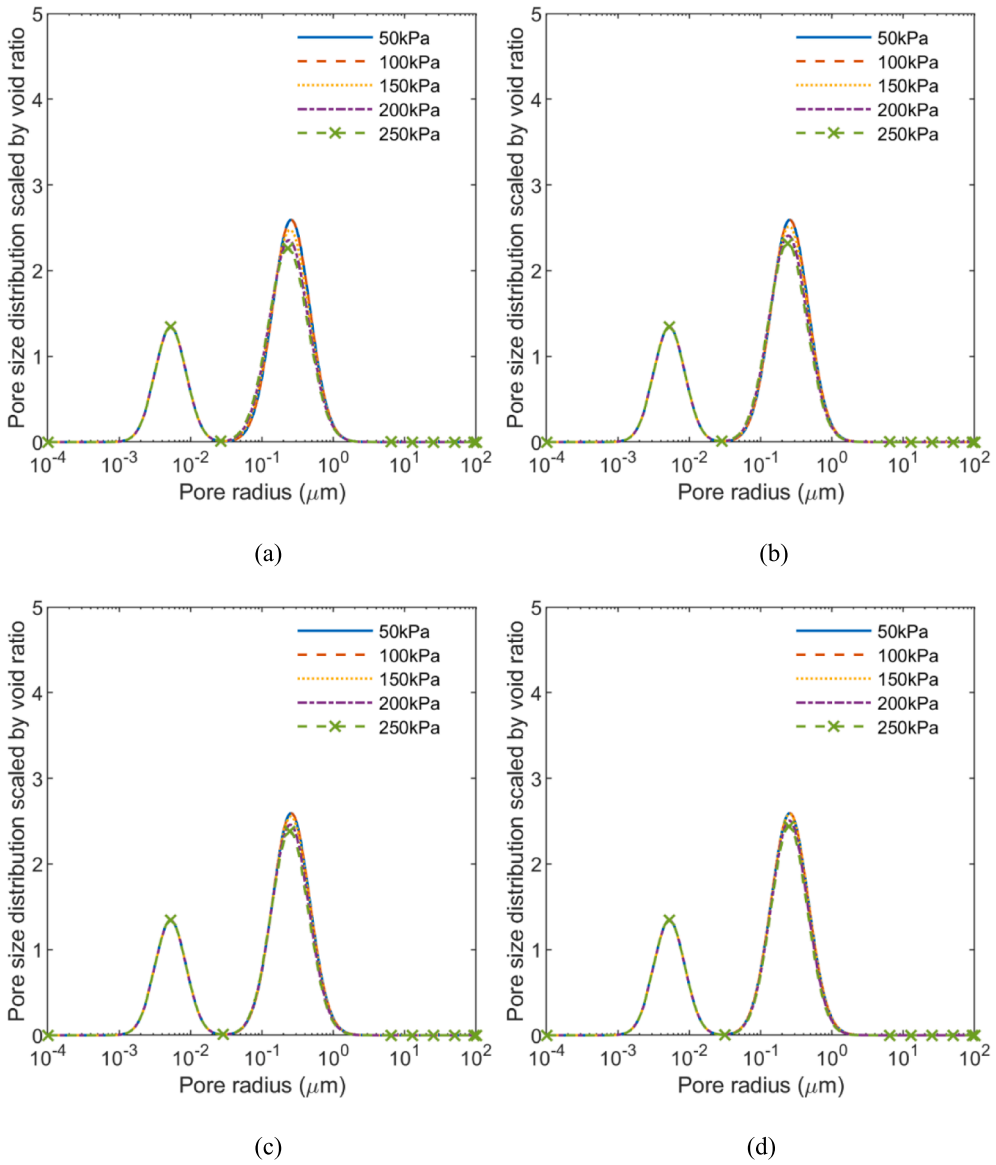

Fig. 14. Evolution of pore size distributions under various K_3^1: (a)$K_3^1 = -0.24$; (b)$K_3^1 = -0.12$; (c)$K_3^1 = 0$; (d)$K_3^1 = 0.12$.

where the subscripts 1 and 2 represent inter-aggregate pores and intra-aggregate pores, respectively. Table 3 also presents the initial PSD. Since the PSD is scaled by the void ratio and has a format of log-normal distribution, then it can be found that:

$$\int_0^{+\infty} f(r)\mathrm{d}r = a_1 + a_2 \tag{31}$$

5.1. Model response

Fig. 3 presents the evolution of the PSD during the isotropic loading. All these PSDs have a bimodal shape where both inter-aggregate PSDs (for macropores) and intra-aggregate PSDs (for micropores) can be easily distinguished. The peak density of inter-aggregate PSDs occurs at around 0.35microns while that of intra-aggregate PSDs is at about 0.005 μm. The highest density of inter-aggregate PSDs is about 2.7 and that of intra-aggregate PSDs is about 1.40. During the isotropic loading, peak densities of the inter-aggregate PSDs drop and the dominant pore size moves left, which is related to the compression and volume decrease of macropores. For the intra-aggregate PSDs, since the evolutional parameters were assumed to be zero, these PSDs remain almost constant in shapes and positions during the loading. This style of PSDs evolution reflects the trends observed in reported experimental data. According to the experimental results from various researchers (Burton et al., 2014; Li and Zhang, 2009; Sridharan et al., 1971; Tanaka et al., 2003; Thom et al., 2007), volume change mainly derives from the compression of macropores such that a downward movement of the inter-aggregate PSD is often witnessed. Due to the reduction of macropores during compression, the dominant pore size can also decrease, as indicated by the left movement of inter-aggregate PSD.

Fig. 4 shows the comparison between modelling and experimental results reported by (Lloret-Cabot et al., 2013; Sivakumar, 1993). For the modelling result, the χ^* remains almost constant at the early stage of loading and then starts to increase after yielding on both LC and SD yield surfaces. The evolution of χ^* is similar to the change of degree of saturation but χ^* is always smaller than the degree of saturation, which is consistent with the findings reported by Vaunat and Casini (2017). Yielding on both LC and SD yield surfaces occurs at a net mean stress of approximately 130 kPa. At the yielding point, the simulated behaviour is sharper in nature that the experimental results. This can be attributed to the adoption of the classical elasto-plasticity theory (Lloret-Cabot et al., 2013). Generally, the proposed model succeeds in predicting the

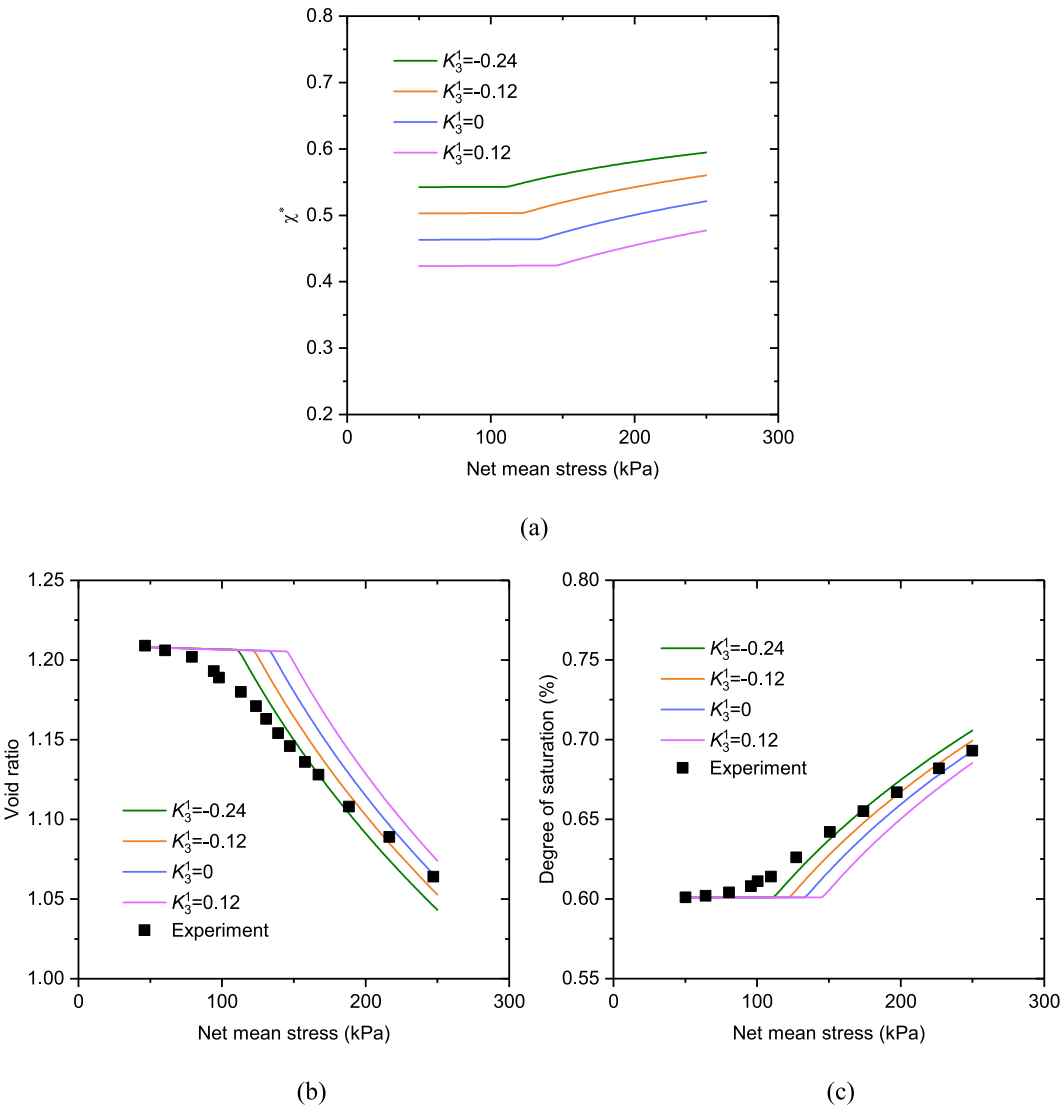

Fig. 15. Model sensitivity to K_3^1: (a) Bishop's effective stress coefficient; (b) Void ratio; (c) Degree of saturation.

development of both void ratio and degree of saturation based on the selected model parameters.

Fig. 3 and Fig. 4 highlight the most significant contribution of the proposed model, which is that the microstructurally based model can not only satisfactorily reproduce the hydro-mechanical behaviour based on the idealized parameters but can also represent the evolution of pore size distributions, something which is not possible in non-microstructure based models. Since pore size distribution is one of the most important pieces of information on the particle rearrangement in particulate systems and can be applied to many areas such as volume change, water retention and permeability, the proposed model has significant potential in engineering application. For example, the pore size distribution can be used to estimate the soil water characteristic curve (SWCC) based on the relationship between water content and pore volume (Fredlund and Xing, 1994; Simms and Yanful, 2004). It should be noted that an SWCC obtained from a specific pore size distribution can only represent the water retention behaviour when the microstructure is unchanged, which means the void ratio and dry density remains constant with suction. However, since the proposed model can predict the evolution of PSD, it is also capable of representing the evolution of SWCC when the microstructure alters during loading.

Fig. 5 presents a comparison of the SWCCs of Speswhite kaolin established from the proposed model between modelling results and the reported experimental results (Sivakumar, 1993; Tarantino, 2010, 2009). The modelling results indicate that the SWCC shift to the right when the void ratio decreases during isotropic loading. Larger pores are compressed during loading and water is stored in relatively smaller pores; a higher suction is thus required to evacuate the water from the smaller pores. The modelling results reproduced the changing tendency of degree of saturation with suction for the clay. The differences between the modelling and experimental results in Fig. 5 are attributed to: (1) the modelled SWCCs are obtained based on the estimated initial pore size distribution and evolutional parameters (Table 2) instead of the actual experimental pore size distributions; (2) the experimental SWCCs have different initial void ratios (dry densities) compared with the modelled SWCCs; (3) samples prepared at the same dry density and different water content produce different fabric and structure (Lambe and Whitman, 1991) and hence different pore-size distribution and SWCCs. (4) methods used for sample preparation will also affect the microstructure of soils even if the void ratio (dry density) is prepared to the same level, leading to difference in SWCC. Additionally, saturation and mechanical loading will have different impact on the evolution of pore size distribution (Li and Zhang, 2009; Wang et al., 2020). Therefore, two samples of the same soil prepared to the same void ratio will not necessarily have the same microstructure, resulting in the difference in SWCC. In this study, the modelled SWCCs are actually based on the evolution of

microstructure during unsaturated isotropic loading while the experimental results are for compacted samples.

5.2. Sensitivity analysis

Compared with using degree of saturation as the Bishop's effective stress coefficient, the PSD-dependent χ^* is significantly more complex. Firstly, because of the limitation of MIP in typical testing ranges (Gramegna, 2022; Li and Zhang, 2009; Tanaka et al., 2003), the PSDs obtained from MIP should not be considered as fully representative of the actual PSDs of soils, which may lead to inaccuracy in calculating χ^*. Secondly, due to the heterogeneity of soils and the irregularity of experimental PSDs, it is possible that the shape-fitting parameters for PSDs and evolutional parameters can be of variation for the same soil sample. Therefore, it is necessary to carry out model sensitivity analysis of the PSD-related parameters to evaluate the reliability of using MIP as the source of obtaining PSDs. In the following sections the sensitivity of the model to the various parameters used in the adopted PSD relationship is considered.

5.2.1. Sensitivity analysis (a_2)

The parameter a_2 represents the volumetric proportion of intra-aggregate pores. Since the summation of a_1 and a_2 is equal to the void ratio, the increase of a_2 will lead to a higher proportion of intra-aggregate pores compared to inter-aggregate pores. A_2 values of 0.001, 0.01, 0.1 and 0.5 are considered (the other parameters remain the same as indicated in Table.3), the resulting PSDs and their evolution are shown in Fig. 6. Due to the zero value of evolutional parameters, the intra-aggregate PSDs remain constant regardless of each proportion. For inter-aggregate PSDs, it can be seen that there is still a similar downward movement of the peak densities. Fig. 7 presents the simulated hydro-mechanical behaviour and its comparison with the experimental results. In terms of χ^*, a significant increase can be witnessed with the increase of a_2. χ^* still has a similar changing tendency as the degree of saturation but χ^* is always smaller than the degree of saturation at each net mean stress. Despite the significant variation of χ^*, the change of a_2 does not have a profound impact on the hydro-mechanical behaviour. The difference in the void ratio and the degree of saturation is low compared to the large disparity among the parameters a_2. Therefore, the newly introduced model is not particularly sensitive to the proportion of intra-aggregate PSDs.

5.2.2. Sensitivity analysis (σ_1)

The parameter σ_1 is the standard deviation of a log-normal distribution. σ_1 can affect the width and the pore size at peak density of the inter-aggregate PSD. Fig. 8 presents the PSDs and their evolution at various values of σ_1 (0.3,0.6,1.2 and 2.4) (the other parameters remain the same as indicated in Table.3). The PSDs show less bimodality when σ_1 increases tending towards a unimodal form. During loading, the inter-aggregate peaks in the PSDs reduce. As shown in Fig. 9, there is a slight impact on χ^* (the larger the σ_1 is, the smaller the χ^* will be), the void ratio and the degree of saturation when the σ_1 decreases from 2.4 to 0.6. When the σ_1 is 0.3, a sharp increase of χ^* can be seen, which can lead to a much larger effective stress at a specific net mean stress. Therefore, the difference among simulated results increases and the yielding on both LC and SD yield surfaces occurs at a lower net mean stress.

5.2.3. Sensitivity analysis (μ_1)

The parameter μ_1 affects the peak density and the position of pore size at peak density for inter-aggregate PSDs. The PSDs under various values of μ_1 (-2, -1, -0.5 and -0.25) are presented in Fig. 10. The other parameters remain the same as indicated in Table.3. It can be seen that the PSDs which have a higher μ_1 will have a lower peak density while its position moves to the right. The decrease of peak density is due to the compression of macropores. However, the evolution of PSDs become less significant with the increase of the parameter μ_1, especially when μ_1 is higher than -1. This is because χ^* is at a very low level (see Fig. 11(a)) and the effective stress is not large enough to generate plastic deformation. Especially when μ_1 is -0.25, negative and unreasonable χ^* occurs (the contribution of suction to effective stress is 0 or positive (Wheeler et al., 2003)). According to Fig. 11, the model shows great sensitivity to the parameter μ_1. Significant disparity between experimental results and simulated results can be seen when μ_1 varies from -2. A higher μ_1 will bring about a much lower χ^*, an obvious delay in yielding, and a less change in the void ratio and the degree of saturation.

5.2.4. Sensitivity analysis (K_2^1)

The parameter K_2^1 controls the evolution of the μ_1 with changes in void ratio. Since the void ratio always decreases during an isotropic loading path, the μ_1 will increase in this path when K_2^1 is negative but will decrease if K_2^1 is positive. In this sensitivity analysis, K_2^1 is selected as 0.15, 0.3, 0.6 and 1.2. As shown in Fig. 12, it still can be observed that the peak density drops down but the difference at each K_2^1 among PSDs narrows with the increase of K_2^1. From Fig. 13, the model, as expected, is also sensitive to the parameter K_2^1. With the increase of K_2^1, there is less volumetric change and less degree of saturation change due to the sharp decrease in χ^*.

5.2.5. Sensitivity analysis (K_3^1)

The parameter K_3^1 has an impact on the evolution of the standard deviation. A negative K_3^1 will lead to the increase of standard deviation during the loading while a positive K_3^1 will induce the decrease of the standard deviation. The movement of the PSDs under various K_3^1 (-0.24, -0.12, 0, 0.12) is similar to the movement previously stated (see Fig. 14). As shown in Fig. 15, the change of K_3^1 will moderately affect the simulated hydro-mechanical behaviour. At K_3^1 of -0.24, the effective stress coefficient χ^* is at the highest level and there is larger change in the void ratio and the degree of saturation compared with experimental result. With the increase of K_3^1, a smaller χ^* can be seen during isotropic loading, as a result of which the changes of void ratio and degree of saturation slow down. In general, the model shows some moderate sensitivity to K_3^1.

6. Conclusion

A constitutive model considering the interaction between evolution of microstructure and hydro-mechanical behaviour of unsaturated soils was proposed and evaluated in this paper. The model for the first time adopts a PSD-dependent Bishop's effective stress coefficient in an existing hydro-mechanical coupled model. The model is able to represent the hydro-mechanical behaviour and microstructural evolution within the same framework and has the potential of studying SWCC and the effects of microstructure in other multi-coupling behaviour of soils. Model response and sensitivity analysis based on the published experiments on Speswhite kaolin (isotropic loading) and idealized assumptions on pore size distributions were undertaken to evaluate the performance of the model and the reliability of using PSDs obtained from MIP. According to the simulated results, the following conclusions can be drawn:

(1) According to the result from the model response, the model is able to reproduce the hydro-mechanical behaviour of unsaturated soils based on published hydro-mechanical parameters and assumed pore size distribution parameters of Speswhite kaolin. This also indicates the potential of this model to be applied to predicting the behaviour of other soils.
(2) Compared with other constitutive models that do not consider the microstructure or only consider the microstructure in an indirect way, an important contribution of this model is that it can

directly consider the microstructure though the pore size distribution and represent the microstructural evolution.

(3) According to the sensitivity analysis, the model is not sensitive to the volume proportion of the intra-aggregate pores (micropores) but is sensitive to the properties of the inter-aggregate pores (macropores) and the evolutional parameters. However, the degree of sensitivity to inter-aggregate pores properties is not excessively high traditional methods for obtaining PSDs such as Mercury Intrusion Porosimetry (MIP) can be used to provide PSD-related parameters for this model.

This study is limited to the consideration of isotropic loading paths based on a combination of both experimentally obtained and assumed parameters (due to the lack of some detailed experimental evidence such as evolution of PSDs during loading). Despite this, model performance suggests that use of a PSD-dependent χ^* warrants further study. This future work should include MIP tests on triaxial samples that have experienced shearing load paths to different axial strains under controlled conditions, so as to allow fuller validation of the model.

7. Data availability statement

The datasets generated during this study are available from the corresponding author upon reasonable request.

CRediT authorship contribution statement

Tianchi Wu: Writing – original draft, Software, Methodology, Investigation, Data curation, Conceptualization. **Peter Cleall:** Writing – review & editing, Supervision, Methodology, Conceptualization. **Snehasis Tripathy:** Writing – review & editing, Supervision, Methodology, Conceptualization.

Declaration of competing interest

The authors declare that they have no known competing financial interests or personal relationships that could have appeared to influence the work reported in this paper.

Data availability

Data will be made available on request.

Acknowledgement

This work was funded by the China Scholarship Council (CSC) from the Ministry of Education of P.R. China (CSC202007090010).

References

Alekseeva, T.V., 2007. Soil microstructure and factors of its formation. Eurasian Soil Sci. 40, 649–659. https://doi.org/10.1134/S1064229307060063.

Al-Mukhtar, M., Khattab, S., Alcover, J.-F., 2012. Microstructure and geotechnical properties of lime-treated expansive clayey soil. Eng. Geol. 139, 17–27. https://doi.org/10.1016/j.enggeo.2012.04.004.

Alonso, E.E., Gens, A., Josa, A., 1990. A constitutive model for partially saturated soils. Géotechnique 40, 405–430. https://doi.org/10.1680/geot.1990.40.3.405.

Alonso, E.E., Pereira, J.-M., Vaunat, J., Olivella, S., 2010. A microstructurally based effective stress for unsaturated soils. Géotechnique 60, 913–925. https://doi.org/10.1680/geot.8.P.002.

Alonso, E.E., Pinyol, N.M., Gens, A., 2013. Compacted soil behaviour: initial state, structure and constitutive modelling. Géotechnique 63, 463. https://doi.org/10.1680/geot.11.P.134.

Bai, B., Xu, T., Nie, Q., Li, P., 2020. Temperature-driven migration of heavy metal Pb2+ along with moisture movement in unsaturated soils. Int. J. Heat Mass Transf. 153, 119573. https://doi.org/10.1016/j.ijheatmasstransfer.2020.119573.

Bai, B., Zhou, R., Cai, G., Hu, W., Yang, G., 2021. Coupled thermo-hydro-mechanical mechanism in view of the soil particle rearrangement of granular thermodynamics. Comput. Geotech. 137, 104272. https://doi.org/10.1016/j.compgeo.2021.104272.

Belnap, J., Gardner, J.S., 1993. Soil microstructure in soils of the Colorado Plateau: the role of the cyanobacterium Microcoleus vaginatus. Gt. Basin Nat. 53, 6.

Bishop, A.W., 1959. The Principle of Effective Stress. Tek. Ukebl. 39, 859–863.

Burger, C.A., Shackelford, C.D., 2001. Evaluating dual porosity of pelletized diatomaceous earth using bimodal soil-water characteristic curve functions. Can. Geotech. J. 38, 53–66.

Burton, G.J., Sheng, D., Campbell, C., 2014. Bimodal pore size distribution of a high-plasticity compacted clay. Géotechnique Lett. 4, 88–93. https://doi.org/10.1680/geolett.14.00003.

Cai, G.Q., Wang, Y.N., Zhou, A.N., Zhao, C.G., 2018. A microstructure-dependent hydro-mechanical coupled constitutive model for unsaturated soils. Chin. J. Geotech. Eng. 40, 618–624. https://doi.org/10.11779/CJGE201804005.

Cai, G., Zhou, A., Liu, Y., Xu, R., Zhao, C., 2020. Soil water retention behavior and microstructure evolution of lateritic soil in the suction range of 0–286.7MPa. Acta Geotech. 15, 3327–3341. https://doi.org/10.1007/s11440-020-01011-w.

Davies, M.C.R., Newson, T.A., 1992. A critical state constitutive model for anisotropic soil. In: Predictive Soil Mechanics. Thomas Telford Publishing, pp. 219–229. https://doi.org/10.1680/psm.19164.0014.

Delage, P., Audiguier, M., Cui, Y.-J., Howat, M.D., 1996. Microstructure of a compacted silt. Can. Geotech. J. 33, 150–158. https://doi.org/10.1139/t96-030.

Delage, P., Lefebvre, G., 1984. Study of the structure of a sensitive Champlain clay and of its evolution during consolidation. Can. Geotech. J. 21, 21–35. https://doi.org/10.1139/t84-003.

Della Vecchia, G., Dieudonné, A.-C., Jommi, C., Charlier, R., 2015. Accounting for evolving pore size distribution in water retention models for compacted clays. Int. J. Numer. Anal. Meth. Geomech. 39, 702–723. https://doi.org/10.1002/nag.2326.

Fredlund, D.G., Morgenstern, N.R., 1977. Stress State Variables for Unsaturated Soils. J. Geotech. Eng. Div. 103, 447–466. https://doi.org/10.1061/AJGEB6.0000423.

Fredlund, D.G., Xing, A., 1994. Equations for the soil-water characteristic curve. Can. Geotech. J. 31, 521–532. https://doi.org/10.1139/t94-061.

Fredlund, D.G., Morgenstern, N.R., Widger, R.A., 1978. The shear strength of unsaturated soils. Can. Geotech. J. 15, 313–321. https://doi.org/10.1139/t78-029.

Fredlund, D.G., Rahardjo, H., 1993. Soil mechanics for unsaturated soils. John Wiley & Sons.

Gallipoli, D., Wheeler, S.J., Karstunen, M., 2003. Modelling the variation of degree of saturation in a deformable unsaturated soil. Géotechnique 53, 105–112. https://doi.org/10.1680/geot.2003.53.1.105.

Gane, P.A., Ridgway, C.J., Lehtinen, E., Valiullin, R., Furo, I., Schoelkopf, J., Paulapuro, H., Daicic, J., 2004. Comparison of NMR cryoporometry, mercury intrusion porosimetry, and DSC thermoporosimetry in characterizing pore size distributions of compressed finely ground calcium carbonate structures. Ind. Eng. Chem. Res. 43, 7920–7927. https://doi.org/10.1021/ie049448p.

Gao, Q.-F., Jrad, M., Hattab, M., Fleureau, J.-M., Ameur, L.I., 2020. Pore morphology, porosity, and pore size distribution in kaolinitic remolded clays under triaxial loading. Int. J. Geomech. 20, 04020057. https://doi.org/10.1061/(ASCE)GM.1943-5622.0001682.

Gens, A., Sánchez, M., Sheng, D., 2006. On constitutive modelling of unsaturated soils. Acta Geotech. 1, 137–147. https://doi.org/10.1007/s11440-006-0013-9.

Ghabezloo, S., Nikooee, E., Habibagahi, G., Mirghaffari, R., 2021. Determination of soil pore size distribution: Application of a new model for soil porous structure 7.

Gramegna, L., 2022. Pore size distribution evolution in pellets based bentonite hydration: comparison between experimental and numerical results. Eng. Geol. 304, 106700. https://doi.org/10.1016/j.enggeo.2022.106700.

Houlsby, G.T., 1997. The work input to an unsaturated granular material. Geotechnique 47, 193–196. https://doi.org/10.1680/geot.1997.47.1.193.

Hu, R.L., Yeung, M.R., Lee, C.F., Wang, S.J., 2001. Mechanical behavior and microstructural variation of loess under dynamic compaction. Eng. Geol. 59, 203–217. https://doi.org/10.1016/S0013-7952(00)00074-0.

Izdebska-Mucha, D., Trzciński, J., 2008. Effects of petroleum pollution on clay soil microstructure.

Izdebska-Mucha, D., TrzcińSk, J., Żbik, M.S., Frost, R.L., 2011. Influence of hydrocarbon contamination on clay soil microstructure. Clay Miner. 46, 47–58. https://doi.org/10.1180/claymin.2011.046.1.47.

Jiang, Y., Einav, I., Liu, M., 2017. A thermodynamic treatment of partially saturated soils revealing the structure of effective stress. J. Mech. Phys. Solids 100, 131–146. https://doi.org/10.1016/j.jmps.2016.11.018.

Khalili, N., Habte, M.A., Zargarbashi, S., 2008. A fully coupled flow deformation model for cyclic analysis of unsaturated soils including hydraulic and mechanical hystereses. Comput. Geotech., Special Issue on Unsaturated Soils: Models, Algorithms and Applications 35, 872–889. doi: 10.1016/j.compgeo.2008.08.003.

Lambe, T W, Whitman, R V, 1991. Soil mechanics[M]. John Wiley & Sons.

Lawrence, G.P., 1978. Stability of soil pores during mercury intrusion porosimetry. J. Soil Sci. 29, 299–304. https://doi.org/10.1111/j.1365-2389.1978.tb00777.x.

Li, P., Shao, S., Vanapalli, S.K., 2020. Characterizing and modeling the pore-size distribution evolution of a compacted loess during consolidation and shearing. J. Soil. Sediment. 20, 2855–2867. https://doi.org/10.1007/s11368-020-02621-3.

Li, P., Shao, S., Xiao, T., Zhu, D., 2021. Pore-size distribution evolution of intact, compacted, and saturated loess from china during consolidation and shearing. Adv. Civ. Eng. 2021, e6644471.

Li, Y., Vanapalli, S.K., 2021. A novel modeling method for the bimodal soil-water characteristic curve. Comput. Geotech. 138, 104318. https://doi.org/10.1016/j.compgeo.2021.104318.

Li, X., Zhang, L.M., 2009. Characterization of dual-structure pore-size distribution of soil. Can. Geotech. J. 46, 129–141. https://doi.org/10.1139/T08-110.

Lloret, A., Villar, M.V., Sánchez, M., Gens, A., Pintado, X., Alonso, E.E., 2003. Mechanical behaviour of heavily compacted bentonite under high suction changes. Géotechnique 53, 27–40. https://doi.org/10.1680/geot.2003.53.1.27.

Lloret-Cabot, M., Sánchez, M., Wheeler, S.J., 2013. Formulation of a three-dimensional constitutive model for unsaturated soils incorporating mechanical-water retention couplings. Int. J. Numer. Anal. Meth. Geomech. 37, 3008–3035. https://doi.org/10.1002/nag.2176.

Marshall, T.J., Holmes, J.W., Rose, C.W., 1996. Soil Physics. Cambridge University Press.

Musso, G., Azizi, A., Jommi, C., 2020. A microstructure-based elastoplastic model to describe the behaviour of a compacted clayey silt in isotropic and triaxial compression. Can. Geotech. J. 57, 1025–1043. https://doi.org/10.1139/cgj-2019-0176.

Nagpal, N.K., Boersma, L., Debacker, L.W., 1972. Pore size distributions of soils from mercury intrusion porosimeter data. Soil Sci. Soc. Am. J. 4. https://doi.org/10.2136/sssaj1972.03615995003600020019x.

Ng, C.W.W., Sadeghi, H., Jafarzadeh, F., Sadeghi, M., Zhou, C., Baghbanrezvan, S., 2019. Effect of microstructure on shear strength and dilatancy of unsaturated loess at high suctions. Can. Geotech. J. https://doi.org/10.1139/cgj-2018-0592.

Nikooee, E., Habibagahi, G., Hassanizadeh, S.M., Ghahramani, A., 2013. Effective stress in unsaturated soils: a thermodynamic approach based on the interfacial energy and hydromechanical coupling. Transp. Porous Media 96, 369–396. https://doi.org/10.1007/s11242-012-0093-y.

Ninjgarav, E., Chung, S.G., Jang, W., Ryu, C.K., 2007. Pore size distribution of pusan clay measured by mercury intrusion porosimetry. KSCE J. Civ. Eng. 11, 133–139.

Niu, G., Cui, Y.-J., Pereira, J.-M., Shao, L., Sun, D., 2021. Determining bishop's parameter χ based on pore-size distribution. Géotechnique Lett. 11, 74–79. https://doi.org/10.1680/jgele.20.00095.

Nuth, M., Laloui, L., 2008. Effective stress concept in unsaturated soils: clarification and validation of a unified framework. Int. J. Numer. Anal. Meth. Geomech. 32, 771–801. https://doi.org/10.1002/nag.645.

Oualmakran, M., Mercatoris, B.C.N., François, B., 2016. Pore-size distribution of a compacted silty soil after compaction, saturation, and loading. Can. Geotech. J. 53, 1902–1909. https://doi.org/10.1139/cgj-2016-0184.

Pasha, A.Y., Khoshghalb, A., Khalili, N., 2017. Hysteretic model for the evolution of water retention curve with void ratio. J. Eng. Mech. 143, 04017030. https://doi.org/10.1061/(ASCE)EM.1943-7889.0001238.

Qian, J., Lin, Z., Shi, Z., 2022. Experimental and modeling study of water-retention behavior of fine-grained soils with dual-porosity structures. Acta Geotech. https://doi.org/10.1007/s11440-022-01483-y.

Rahardjo, H., Cong Thang, N., Kim, Y., Leong, E.-C., 2018. Unsaturated elasto-plastic constitutive equations for compacted kaolin under consolidated drained and shearing-infiltration conditions. Soils Found. 58, 534–546. https://doi.org/10.1016/j.sandf.2018.02.019.

Romano, N., Nasta, P., Severino, G., Hopmans, J.W., 2011. Using bimodal lognormal functions to describe soil hydraulic properties. Soil Sci. Soc. Am. J. 75, 468–480. https://doi.org/10.2136/sssaj2010.0084.

Russell, A.r., Buzzi, O., 2012. A fractal basis for soil-water characteristics curves with hydraulic hysteresis. Géotechnique 62, 269–274. https://doi.org/10.1680/geot.10.P.119.

Sánchez, M., Gens, A., Guimaraes, L., Olivella, S., 2001. Generalized plasticity model for THM simulations involving expansive clays. In: Proceedings of the 6th Int. Workshop on Key Issues in Waste Isolation Research. Presented at the the 6th Int. Workshop on Key Issues in Waste Isolation Research, pp. 28–30.

Sánchez, M., Gens, A., Guimarães, L. do N., Olivella, S., 2005. A double structure generalized plasticity model for expansive materials. Int. J. Numer. Anal. Meth. Geomech. 29, 751–787. https://doi.org/10.1002/nag.434.

Satyanaga, A., 2013. Water characteristic curve of soil with bimodal grain-size distribution. Comput. Geotech. 48, 51–61. https://doi.org/10.1016/j.compgeo.2012.09.008.

Sheng, D., Sloan, S.W., Gens, A., 2004. A constitutive model for unsaturated soils: thermomechanical and computational aspects. Comput. Mech. 33, 453–465.

Sheng, D., Zhou, A.-N., 2011. Coupling hydraulic with mechanical models for unsaturated soils. Can. Geotech. J. 48, 826–840.

Simms, P.H., Yanful, E.K., 2004. Estimation of soil-water characteristic curve of clayey till using measured pore-size distributions. J. Environ. Eng. 130, 847–854. https://doi.org/10.1061/(ASCE)0733-9372(2004)130:8(847).

Sivakumar, V., 1993. A critical state framework for unsaturated soil. University of Sheffield (phd).

Sridharan, A., Altschaeffl, A.G., Diamond, S., 1971. Pore size distribution studies. J. Soil Mech. Found. Div. 97, 771–787. https://doi.org/10.1061/JSFEAQ.0001595.

Tanaka, H., Shiwakoti, D.R., Omukai, N., Rito, F., Locat, J., Tanaka, M., 2003. Pore size distribution of clayey soils measured by mercury intrusion porosimetry and its relation to hydraulic conductivity. Soils Found. 43, 63–73. https://doi.org/10.3208/sandf.43.6_63.

Tarantino, A., 2009. A water retention model for deformable soils. Géotechnique 59, 751–762. https://doi.org/10.1680/geot.7.00118.

Tarantino, A., 2010. Unsaturated soils: compacted versus reconstituted states. Presented at the 5th International Conference on Unsaturated Soil.

Thom, R., Sivakumar, R., Sivakumar, V., Murray, E.J., Mackinnon, P., 2007. Pore size distribution of unsaturated compacted kaolin: the initial states and final states following saturation. Géotechnique 57, 469–474. https://doi.org/10.1680/geot.2007.57.5.469.

Tripathy, S., Tadza, M.Y.M., Thomas, H.R., 2014. Soil-water characteristic curves of clays. Can. Geotech. J. 51, 869–883. https://doi.org/10.1139/cgj-2013-0089.

Tsuji, G.Y., Watanabe, R.T., Sakai, W.S., 1975. Influence of soil microstructure on water characteristics of selected hawaiian soils 1. Soil Sci. Soc. Am. J. 39, 28–33. https://doi.org/10.2136/sssaj1975.03615995003900010011x.

Vaunat, J., Casini, F., 2017. A procedure for the direct determination of Bishop's χ parameter from changes in pore size distribution. Géotechnique 67, 631–636. https://doi.org/10.1680/jgeot.15.T.016.

Wang, M., Bai, X., 2012. Collapse Property and Microstructure of Loess. Adv. Unsaturated Soil Seepage Environ. Geotech. 111–118. https://doi.org/10.1061/40860(192)10.

Wang, J.-D., Li, P., Ma, Y., Vanapalli, S.K., 2019. Evolution of pore-size distribution of intact loess and remolded loess due to consolidation. J. Soil. Sediment. 19, 1226–1238. https://doi.org/10.1007/s11368-018-2136-7.

Wang, J.-D., Li, P., Ma, Y., Vanapalli, S.K., Wang, X.-G., 2020. Change in pore-size distribution of collapsible loess due to loading and inundating. Acta Geotech. 15, 1081–1094. https://doi.org/10.1007/s11440-019-00815-9.

Wang, Y., Yang, H., Jing, X., 2021. Structural characteristics of natural loess in Northwest China and its effect on shear behavior. Geotech. Geol. Eng. 39, 65–78. https://doi.org/10.1007/s10706-020-01420-4.

Washburn, E.W., 1921. The dynamics of capillary flow. Phys. Rev. 17, 273–283. https://doi.org/10.1103/PhysRev.17.273.

Wheeler, S.J., Sharma, R.S., Buisson, M.S.R., 2003. Coupling of hydraulic hysteresis and stress–strain behaviour in unsaturated soils. Géotechnique 53, 41–54. https://doi.org/10.1680/geot.2003.53.1.41.

Woignier, T., Morell, M., Morell, O., Duffours, L., Soler, A., 2011. Low water transport in fractal microstructure of tropical soils: application to chlordecone pesticide trapping. Ecohydrol. Hydrobiol. 11, 121–127. https://doi.org/10.2478/v10104-011-0035-2.

Wu, T., Cai, G., Cleall, P., Tripathy, S., 2022. Microstructurally related model for predicting behavior of unsaturated soils with double porosity in triaxial space. Int. J. Geomech. 22, 04022216. https://doi.org/10.1061/(ASCE)GM.1943-5622.0002569.

Yong, R.N., 2003. Influence of microstructural features on water, ion diffusion and transport in clay soils. Appl. Clay Sci., Clay Microstructure. In: Proceedings of a Workshop held in Lund, Sweden, 15-17 October 2002 23, 3–13. doi: 10.1016/S0169-1317(03)00081-4.

Yu, C.Y., Chow, J.K., Wang, Y.-H., 2016. Pore-size changes and responses of kaolinite with different structures subject to consolidation and shearing. Eng. Geol. 202, 122–131. https://doi.org/10.1016/j.enggeo.2016.01.007.

Zhang, Y., 2005. The microstructure and formation of biological soil crusts in their early developmental stage. Chin. Sci. Bull. 50, 117–121. https://doi.org/10.1007/BF02897513.

Zhang, C., Lu, N., 2020. Unified effective stress equation for soil. J. Eng. Mech. 146, 04019135. https://doi.org/10.1061/(ASCE)EM.1943-7889.0001718.

Zhou, H., Mooney, S.J., Peng, X., 2017. Bimodal soil pore structure investigated by a combined soil water retention curve and X-Ray computed tomography approach. Soil Sci. Soc. Am. J. 81, 1270–1278. https://doi.org/10.2136/sssaj2016.10.0338.